Atom-Thick Membranes for Water Purification and Blue Energy Harvesting

Dawid Pakulski, Wlodzimierz Czepa, Stefano del Buffa, Artur Ciesielski, Paolo Samori

WILEY-VCH

DOI: 10.1002/ ((please add manuscript number))

Article type: Review

Atom-thick membranes for water purification and blue energy harvesting

Dawid Pakulski, Włodzimierz Czepa, Stefano Del Buffa, Artur Ciesielski, Paolo Samorì**

D. Pakulski, Dr. A. Ciesielski, Dr. Stefano Del Buffa, Prof. P. Samorì

Université de Strasbourg, CNRS, ISIS

8 allée Gaspard Monge, 67000 Strasbourg, France.

E-mail: ciesielski@unistra.fr ; samori@unistra.fr

D. Pakulski, W. Czepa, Dr. A. Ciesielski

Centre for Advanced Technologies,

Umultowska 89c, 61614 Poznań, Poland

D. Pakulski, W. Czepa

Faculty of Chemistry, Adam Mickiewicz University

Umultowska 89b, 61614 Poznań, Poland

Keywords: blue energy, pressure retarded osmosis, reversed electrodialysis, 2D materials, atom thick membranes

Abstract

Membrane-based processes such as water purification and harvesting of osmotic power deriving from the difference in salinity between seawater and freshwater, are two strategic research fields holding great promises for overcoming critical global issues like the world growing energy demand, the climate change and the access to clean water. Ultrathin membranes based on two-dimensional materials (2DMs) are particularly suitable for highly selective separation of ions and effective generation of *blue energy*, because of their unique physico-chemical properties and novel transport mechanisms occurring at the nano- and sub-nanometer length scale. However, due to the relatively high costs of fabrication compared to traditional porous membrane materials, their technological transfer towards large-scale applications still remains a great challenge. Herein, we present an overview of the current state-of-the-art in the development of ultrathin membranes based on 2DMs for osmotic power generation and water purification. We discuss several synthetic routes to produce atomically-thin membranes with controlled porosity and we describe in detail their performances, with a particular emphasis on pressure retarded osmosis and reversed electrodialysis methods. In the last section, outlooks and current limitations as well as viable future developments in the field of 2DMs membranes are provided.

1. Introduction

The continous increase of global energy demand and the urgent requirements associated to the growing pollution and climate change are continously stimulating the scientific community towards the development of efficient and reliable technologies, which will make use of renewable energy sources, and eventually replace conventional, exhaustible methods based on fossil fuels.[1] Numerous alternative sources of clean energy have been identified, including wind, bioenergy, solar and water power.[1b] According to the Interntional Energy Agency, the share of renewables in meeting global energy demand is expected to reach 12.4% in 2023, with almost one third of the global electricity power demand being provided by renewable sources.[2] However, the complete replacement of fossil fuels still represents a long-term goal since the limited efficiency associated with the production and storage of electrical power from renewable sources represents, in most cases, a big concern. A remarkable amount of energy has been recently identified in the salinity gradient potential, which allows to harvest so-called *blue energy* by exploiting natural aquatic systems. This form of energy derives from the difference in osmotic pressure that is generated when two aqueous solutions with different salt concentration are separated by a semi-permeable membrane. In order to equilibrate the chemical potential of the solvent in the two reservoirs, water tends to flow from the diluted feed solution (*i.e.*, fresh water) to the more concentrated draw solution (*i.e.*, seawater). The osmotic pressure is defined as the excess hydrostatic pressure which must be applied to overcome this spontaneous stream of solvent through the membrane, according to the well-known Vant'Hoff equation:

$$\Pi = cRT \qquad (1)$$

in which c is the molar concentration of the solution.[3]

The Gibbs free energy released from the spontaneous mixing of ideal solutions of different salinity can be calculated from the difference between the Gibbs free energy of the mixed (G_1) and that of the unmixed (G_2 and G_3) solutions:

$$G = \sum_i \mu_i n_i = \sum_i \mu_i c_i V \quad (2)$$

$$\Delta G_{mix} = G_1 - (G_2 + G_3)$$
$$= \sum_i \mu_i C_i V = \sum_i \left(c_{i,1} V_1 RTlna_{i,1}\right) - \left(c_{i,2} V_2 RTlna_{1,2} + c_{i,3} V_3 RTlna_{i,3}\right) \quad (3)$$

where subscripts 1, 2 and 3 refer to the final mixed solution and to the initial solutions of different salinity, respectively, V is the volume of the solutions and a is the activity of the i^{th} component of the ideal solution.[4] Equation 2 and 3 do not take into account the free energy difference of water (*i.e.*, AG^0_{mix}), which results in an underestimation of <10%.[4]

The osmotic flow can thus be exploited to directly convert ΔG_{mix} to mechanical and electrical work by the controlled mixing of water masses of different salt concentration. Even though salinity gradient potential was overlooked throughout the years, recent investigations have made remarkable advances in *blue energy* generation resulting in few pilot plants installed in Norway, Japan, Italy and Korea.[5] Theoretical calculations based on entropy change report that up to 0.8 kW/m^3 can be effectively harvested at the sea-river interface.[6] Although this amount of energy is much lower than that conventionally produced by burning fossil fuels, several advantages (one and foremost the huge availability of saline water on Earth) make salinity gradient energy an attractive alternative and a promising renewable solution for future's energy harvesting.[7] Effective sourcing of osmotic power requires the establishment of efficient energy-conversion technologies and the continous development of functional materials. Several methodologies to harvest salinity-gradient energy have been developed so far, most of which rely on processes that make use of separation membranes. Among the currently available

options, pressure retarded osmosis (PRO) and reversed electrodialysis (RED) represent two among the most promising and mature technologies. In PRO, a salt-rejecting porous semipermeable membrane is placed in between two solutions with a concentration gradient, allowing for controlled mixing and energy production.[8] Briefly, the volume expansion of the draw solution resulting from the permeation of water from the feed solution through the membrane causes a pressure build-up, which is partially released by an outlet flow powering a hydroturbine that generates electricity.[9] Conversely, RED is based on directional transport of charges driven by Nernst potential, using ion-exchange membranes and directly converting osmotic power in electricity by using suitable electrodes and an external load resistance.[10] Recent progress in this field have enabled to produce power outputs in the range of several W/m^2.[9] A great advantage of PRO and RED methods comes from the fact that both can be applied in natural water reservoir systems such as estuaries[11] and can operate in continous, unlike wind and solar energy harvesting systems. Unfortunately, critical limitations of salinity gradient-based processess result from the osmotic transport across the membranes. In fact, the development of PRO and RED technologies have been practically restricted so far by the lack of membranes able to allow for a sufficient flow, and the energy generated by these systems results to be currently limited by the properties of the adopted membrane. Therefore, a comprehensive understanding of the transport mechanism as well as the search for novel materials result are crucial for the optimization of the whole process and further technological developments in the field. Apart from harvesting *blue energy*, membrane separation processes are also key to another strategic global issue, i.e. water purification. The alarming report recently released by the World Health Organization,[12] with at least 2 billions of people currently using contaminated drinking water and half of the global population expected to live in water-stressed area by 2025, calls for global political actions, but also urges the scientific community to develop efficient materials and accessible technologies for water purification. Because of the inverse scaling of water flow with the membrane's thickness and high

selectivity, two-dimensional materials (2DMs) can offer a new approach over the control of mass transport at the nanoscale, and possibly leading to the emergence of a disruptive technology in the field of membrane science. Since the discovery of graphene in 2004[13] the research in 2DMs has grown exponentially and has heavily influenced many classical fields such as chemistry and condensed physics, as well as interdisciplinary domains like materials science and nanotechnology.[14] The importance of these atomically thin sheets of layered compounds (graphene, transition metal dichalcogenides, boron nitride, MXenes, phosphorene, *etc.*) resides in the fact that their exceptional chemical and physical properties (*e.g.*, photoluminescence, semi-metallic conductivity, semiconducting charcateristics with tuneable band-gaps, extremely high surface-to-volume ratio, *etc.*) are dictated by their dimensionality and can be finely tuned by chemical engineering of their surface, resulting in outstanding materials for fundamental and applied research. Atomically thin membranes have been recently investigated for applications in water desalination and purification,[15] chemical sensing and separation,[16] energy conversion,[6, 9, 17] and gas separation[18] due to the beneficial presence of micropores (pore width <2.0 nm, according to the IUPAC definition) in their ordered lattices that allows for selective transport of molecules and ions with uppermost permeability.[19] Moreover, atomic-scale thickness, chemical resistance and extreme mechanical strength offered by 2DMs all constitute valuable features to be considered in membrane separation processes.[20] This Review aims at summarizing the recent progresses on the use of atomically-thin membranes for water purification and osmotic power harvesting based on 2DMs, and motivating the interest in novel technological developments based on 2DMs-based membranes. Firstly, we will present the currently adopted methods for the fabrication of atom-thick membranes based on graphene, graphene oxide, MoS_2, and related hybrid materials, then we will discuss the performances of the resulting membranes in PRO and RED applications based on the latest scientific literature reports. Aiming at providing a practical, critical overview of the vast research activity and on the latest developments in the field, we will draw particular

attention on what is currently scientifically and technologically feasible in order to highlight the potential impact of salinity gradient as a strategic renewable energy source. Considering the specific subject of this Review, the reader is referred to more general works on polymers[21] and other functional materials (*e.g.*, metal-organic frameworks,[22] zeolites,[23] silica[24]), as well as on *bottom-up* fabrication techniques of meso- and microporous inorganic matrices [19b, 25], used in membrane separation processes.

2. Materials for fabrication of atomically-thin membranes

In general, membranes are thin semi-permeable barriers laying at the basis of a number of separation processes typically achieved through gravity or concentration, salinity, electrical potential, temperature and pressure gradients.[15b, 26] Semi-permeable membranes used, for instance in desalination processes, can be usually classified into three categories based on their composition: inorganic, organic and inorganic-organic hybrids. Ceramic materials (such as SiO_2, Al_2O_3, TiO_2),[27] carbon-based materials (graphene and related layered materials as well as carbon nanotubes)[15d, 20b, 28] and other two dimensional materials (such as MoS_2 and hBN)[20c, 29] all belong to the first class. Organic membranes are composed of polymeric materials, typically polyamide, polyvinyl alcohol, cellulose acetate, polypropylene, polysulfone, polyvinylidene fluoride, and represent the standard of commercially-available technologies.[30] The last group of inorganic-organic hybrid membranes are usually obtained *via* incorporation of inorganic fillers into polymeric matrices, or by the combination of inorganic and organic membranes.[31] In this Review we focus our attention on the recent developments of inorganic membranes based on 2DMs (*i.e.*, graphene (G), graphene oxide (GO), molybdenum disulfide (MoS_2) and on their corresponding organic-inorganic hybrids.

Despite the widespread exploitation of bulky multilayered membranes in *e.g.* desalination process, these materials may suffer from drastic internal concentration polarization (ICP) when they are used in PRO and RED, which significantly reduces the water flux over time, and

therefore also the power density.[9, 32] On the other hand, membranes based on graphene and related 2DMs have recently been considered as a valuable alternative to traditional materials (*e.g.*, in osmotic pressure membranes) due to the fact that water transport through a membrane scales inversely with its thickness.[33] The atomic-level thickness of 2DMs thus makes them the thinnest possible barrier, massively minimizing transport resistance and ultimately maximizing water flux.[15e, 29a]

Another ubiquitous and severe limitation of all membrane-based technologies operating in real conditions (*i.e.*, raw natural acquatic reservoirs or municipal wastewater) is represented by the fouling process, during which pore blocking, cake formation, organic adsorption, inorganic precipitation and biological fouling take place on the membrane surface, ultimately hindering its separation performances and leading to temporary or permanent flux decline.[34] General strategies to prevent membranes fouling typically involve a fine-tuning of the physico-chemical properties of the surface achieved by means of hydrophylic and superhydrophylic coatings, chemical/supramolecular grafting on the surface or adsorption of inorganic particles, as well as pre-treatment of the water reservoirs (*e.g.*, addition of oxidising agents, flocculants, coagulants) or optimization of operative conditions such as pH, temperature, applied pressure and hydrodynamic conditions (*e.g.*, high cross-flow velocity).[35] Interestingly, some 2DMs-based membranes are known to display antifouling characteristics. The incorporation of negatively charged GO in thin film composite membranes, for instance, helps in reducing the adsorption of negatively charged foulants thanks to electrostatic repulsions and the formation of a hydration layer acting as a steric barrier. Furthermore, the hydrophilic nature and low surface roughness, together with the possibility of easily decorating its surface with photoactive metal/metal oxide nanoparticles, provides additional (bio)fouling resistance to GO-based hybrid membranes.[36] Recently, an active layer of CVD graphene transferred onto a commercial PTFE membrane has been shown to display antifouling properties against surfactants and oils, and to succesfully operate in real desalination conditions. In particular,

antifouling properties of graphene are attributed to the decreased hydrophobicity (with respect to pristine PTFE), surface charge neutrality and weak physisorption interactions with the foulant species investigated.[37]

Overall, the ability to precisely control membrane thickness, surface chemistry and micro-meso porosity is crucial for the development of materials to be used in *blue energy* nanogenerators and water purification systems.

The continous progress in advanced fabrication techniques, together with the unparalleled physical and chemical properties of 2DMs such as high surface-to-volume ratio, mechanical strength,[38] chemical robustness[39] and selectivity[16b] have thus paved the way for a new era in the field of membrane separation processes.

2.1. Preparation methods of 2D materials-based membranes

Nanosheets of 2DMs with atomic thickness can be used as main components to produce various separation membranes including porous 2D membranes, layered stacks membranes and hybrid 2D-polymeric membranes (**Figure 1**). The main parameters used to describe and compare the quality of newly prepared membranes are surface morphology, thickness, porosity and pore functionalization, which in turn can selectively affect the mass transport across the membrane. Numerous *top-down* techniques for creating pores of precise dimensions have been developed, and include electron beam irradiation,[40] oxidative etching[18c] and plasma etching.[41] On the other hand, to fabricate layered stacks and hybrid membranes typical methodologies involve phase inversion,[42] interfacial polymerization,[43] electrospinning,[44] blending,[45] surface coating,[46] filtration assisted coating,[15a] and layer-by-layer assembly.[47] The large-scale production of high-quality graphene and related 2D materials is key to develop real technologies and commercial applications. The search for practical and environmental-friendly fabrication methods that could be directly transferred to the industrial level represents a critical

– sometimes limiting – aspect of applied research in 2D materials science and nanotechnology. Along with recent advances in liquid-phase methods based on shear-mixing, ultrasounds, microfluidization or electrochemical exfoliation, roll-to-roll processing holds great promises especially because of the continuous operation mode and the facile integration with ordinary industrial equipment.[48] Kidambi et al.,[49] for instance, has recently described a method for the production of nanoporous atomically thin membranes based on roll-to-roll chemical vapor deposition (CVD) of graphene and subsequent casting of polyether sulfone (PES). The monolayer graphene can be grown at a remarkable speed of 5 cm/min and, after etching of the underlying Cu growth substrate, a large area (>3 cm^2) PES-supported graphene membrane was obtained. In the following section, fundamental mechanisms for the generation of 2DMs-based membranes are briefly summarized and some of the most appealing examples are highlighted.

2.1.1. Porous 2DMs Membranes

In Nature, pores in cell membranes play a fundamental role in signal transduction, osmoregulation, transport of nutrients and fusion of cells. The mechanism of pore formation, although not yet understood in details, requires surmounting the energy barrier (*i.e.*, the entropically unfavorable spatial confinement of water molecules within the pore region) and it is driven by favourable enthalpic protein-protein interactions.[50] In materials science, the controlled formation of pores with defined size in a given material is inherently challenging, with pore density and pores average size mainly being dependent on the coaction of defects nucleation and their growth into larger pores.[51] Various practical approaches for the *top-down* generation of pores within 2D materials have been proposed in the literature.[26e] Single layer graphene (SLG) nanosheets with artificially obtained pores, for instance, could find application in ionic sieving membranes. Molecular dynamics studies presented by Cohen-Tanugi *et al.* indicate that nanoporous graphene can act as a barrier for salt ions (**Figure 2a**) while allowing

the flow water with permeabilities several orders of magnitude higher than existing reversed-osmosis membranes, emphasizing the potential of nanoporous single-layered membranes in desalination process (**Figure 2b**).[15d]

Suk and co-workers further proposed that graphene with a pore size in the range of 1-3 nm would allow ~10% faster water transport through the membrane, compared to thin carbon nanotubes (CNTs membranes).[33] Interestingly, nanoporous few layers graphene membranes with thickness below 10 nm can be produced using low-energy (<10 keV) focused electron beam in a scanning electron microscope (SEM), in the presence of nitrogen gas (**Figure 3a**). N_2 is ionized by the electron beam directly in the SEM chamber, then it chemically interacts with carbon atoms forming cyanogen, a gaseous product that is aspirated by the pump, and leading to the formation of pores on the graphene surface.[52] Despite the low density of pores which can be achieved *via* this method, a fine control over pore formation was demonstrated by varying beam current and gas pressure.

Fischbein and Drndić demonstrated the precise modification of suspended multiayer graphene sheets by exposing the material to the focused electron beam (energy of hundreds of keV) of a transmission electron microscope (TEM).[53] By irradiating a few-layered graphene sheet (ca. five layers) with an electron beam for ~5 s, pores with diameter ~3.5 nm have been generated. Garaj and co-workers reported on a graphene sub-nanometric trans-electrode membrane grown *via* CVD method on nickel surface.[40a] The graphene membrane was placed on a SiN_x/Si substrate chip and nano-sized pores were generated using the electron beam of a TEM. The authors studied the interactions of the membrane with different alkali metal ions solutions by investigating the surface electrochemical behavior, showing multiple opportunities for further modifications and applications of the obtained 2D membrane.

Liu *et al.* presented a method of fabrication based on molybdenum disulfide (MoS_2) sculpted *via* TEM. MoS_2 flakes were first mechanically exfoliated on SiO_2 substrate, then transferred to

a square-shaped opening located on a SiN_x membrane, thermally annealed at 400 °C under H_2/Ar flux and finally subjected to the electron beam drilling with an applied voltage of 200 kV. Pores with size ranging from 2 to 20 nm were obtained on single- and few-layer MoS_2. The authors demonstrated better water-transport behavior and higher performances in detecting DNA translocations of the so-obtained nanoporous MoS_2 membrane with respect to conventional thicker silicon nitride membranes or graphene.[54] Feng *et al.* lately reported on a MoS_2 nanopores as an osmotic nanopower generator.[29b] Both TEM irradiation and electrochemically reaction techniques (ECR) were applied to create a single pore in the MoS_2 nanostructure. Based on the membrane efficiency, it was shown that the osmotically induced current reached 10^6 W m^{-2}, which is approximately three orders of magnitude greater than the value obtained with boron nitride nanotubes,[55] and six orders of magnitude higher than the power density obtained in reversed electrodialysis with classical membranes made of cellulose acetate or polyamide.[9] Recent experimental advances have demonstrated that subnanometer-sized pores in SLG sheets can also be produced by O_2 plasma irradiation, with size and density of the pores increasing with the plasma etching time.

Surwade and co-workers proposed an approach for a controlled formation of pores with diameters ranging from 0.5 to 1 nm with a density of $\approx 10^{10}$ cm^{-2} in a SLG, by using an oxygen plasma-etching process with an etching time of ~1.5 s (**Figure 3b**). [19b] Another approach to generate randomly distributed pores over large areas consists in using oxidative etching. This route considerably enhances the scalability of the process while simoultanesly decreasing the pore size down to the sub-nanometer scale. Liu and co-workers demonstrated that thermal oxidation of graphene and graphite induces the formation of a low density of large pores (>10 nm).[56] Further oxidation at higher temperature (500 °C) caused the etching of pores ranging from 20 to 180 nm in diameter in single-layer graphene, but not in double- and multi-layered sheets. Accordingly, SLG reacts faster and presents randomly distributed etch pits in contrast to natural graphite where nucleation of pores preferentially takes place at point defects. Tao *et*

al. characterized the highly disordered morphology of a SLG sheet, as well as that of a graphitic material, treated in an ozone generator. The presence of ozone and oxygen radicals resulted in nucleation of defects, yielding a high density of pores.[57]

A closely related approach to produce sub-nanometer sized pores in 2DMs membranes involves the creation of reactive spots *via* ion bombardment and their consequent enlargment by chemically oxidative conditions. Hern *et al.* reported a method to create controlled subnanometer-sized pores from 0.24 to 0.40 nm with density exceeding 10^{12} cm^{-2} in large area SLG membranes through chemical oxidation (acidic potassium permanganate) of reactive defects introduced by bombardment with gallium ions (**Figure 3c**).[19a] In turn, Celebi *et al*. reported on the short-exposure dosage of gallium and helium ions as a method to provide fast and exact generation of well-defined pores in graphene, with diameters ranging from <10 nm to 1 μm.[18b] A very large number of pores could be generated by electron beam irradiation at room temperature, however, the obtained pore size is still far from the microporous range (*i.e.*, pore diameter < 2.0 nm) that is needed for selective transport of ions and gases.

2.1.2 Layered stacks and hybrid membranes

Unlike the *top-down* fabrication of pores in a pristine two-dimensional material, recent advances in the production of membranes made of layered stacks of 2DMs with well-defined interlayer distance have shown promising potential in desalination and water purification applications.[15e, 26d, 58] In the following section some of the main processing techniques for the fabrication of stacked layers of 2DMs and hybrid membranes are discussed.

Surface coating is a general process in which 2DMs are mixed with suitable polymer solutions or simply dispersed in a solvent and are being applied on the desired surface. Evaporation of the solvent eventually leads to a stacked coating of nanosheets or a hybrid membrane.[59] Depending on the balance between adhesion with the substrate and cohesion forces among the structural components of the film, the obtained stack of nanosheets can be eventually peeled-

off and used as a self-standing membrane. Due to its simplicity, high throughput and general applicability, this method presents several advanteges for a wide range of applications. Numerous coating strategies have been suggested to assemble 2DMs into layered stacks and to enhance the mechanical properties and separation performances of conventional membranes, including spin/spray coating and drop casting.[60] Therefore, the resulting 2DMs-based membranes possess different thicknesses and surface morphologies correlated to the used coating technique, as well as to the adopted experimental conditions (*i.e.*, concentration and viscosity of the adopted solutions, concentration of 2DMs, wettability and surface chemistry of the underlying substrate, chemical functionalization of the 2DMs, presence of binding agents, drying conditions, *etc*.). For example, by drop casting GO dispersion onto a piece of smooth paper Sun *et al.* were able to obtain free-standing membranes with thickness <10 μm and an interlayer spacing of 8 nm, and investigated their selective ion penetration and water purification properties.[60b] Shen *et al.* described the manufacture of transport mixed membranes *via* surface coating of a polysulfone support with GO nanosheets grafted with hyperbranched polyethyleneimine dispersed in a chitosan matrix cross-linked with polyvinyl amine at high temperature.[46] Chen *et al.* achieved a full control of the interlayer spacing of graphene oxide membranes prepared *via* drop casting by using mono- and di-valent metal ions (K^+, Na^+, Li^+, Ca^{2+}, and Mg^{2+}), with a precision of ~1 Å. [61] This method is based on the strong noncovalent interactions between hydrated cations and the aromatic π-electrons of GO. Experimental results demonstrated that a thin KCl-controlled GO membrane showed a water flux of 0.36 l m^{-2} h^{-1} with effective rejection of sodium ions. Overall, the approach presented by Chen represents a remarkable step forward in GO-based membranes used in water purification processes. Despite these GO membranes also showed a good permselectivity for gases (CO_2/N_2), such direct coating procedure lacks in the precise control over thickness and surface homogeneity. That is the reason why a proper surface coating *via* the direct casting of a polymer solution onto a porous substrate is, in general, a very problematic task.

Spin and spray coating represent widely adopted methods to produce thinner and more organized polymer-based and composite films on various substrates and they are largely employed, for instance, in the production of photoresists in the microelectronics industry and in the paint industry. In a typical spin coating process, a polymer solution or a dispersion is first deposited on a substrate that is then accelerated rapidly to a certain rotation speed. The centrifugal force acting on the liquid film causes it to spread radially and leads to the removal of the excess liquid from the substrate. The thickness of the deposited film diminishes during the rotation of the substrate, until an equilibrium thickness is reached as a consequence of disjoining pressure effects or a dramatic increase in viscosity due to solvent.[62] By a careful selection of operative conditions (*e.g.*, acceleration rate, rotation speed, rotation time, substrate temperature) and experimental parameters (*e.g.*, concentration and viscosity of the solution/dispersion, chemical functionalization of the substrate, etc.) a wide range of homogenous, thin and ultrathin polymer and hybrid films can be obtained.[63] Spray coating is generally considered as the process of forming an aerosol by the action of a pressurized gas impinging upon a liquid flowing through a nozzle, and the application of such aerosol onto a substrate. Depending on the type of material to be processed and its particle size distribution, different nozzle size and geometry as well as different atomization methods can be adopted (high temperature, ultrasounds, hydraulic *vs* pneumatic atomization), the simplest being the dispersion of solid particles in a suitable medium and the use of low-cost instruments such as air brushes or spray cans.

Membranes having a thickness in the 0.1 - 10 μm range and interlayer distance of ~10 Å can be easily produced by spin and spray coating methods.[64] Spin coating results to be particularly suitable for coating flat substrates and has been adopted, for instance, for the surface functionalization of polyacrylonitrile and polysulfone membranes with 2DMs.[65] Pan *et al.* explored MoS_2 nanosheets embedded into a polyether block amide matrix to prepare high-efficiency transport membranes for gasoline desulfurization, using a spin coating method.[65a]

The performances were evaluated using the tiophene/n-ocetane binary mixture as a model, with the hybrid membrane containing 4 wt% MoS_2 resulting the best also in terms of higher permeation flow. A similar methodology has been used by Cao and co-workers to fabricate membranes with a brick-and-mortar cross-sectional structure of pristine and reduced graphene oxide blended with sodium alginate.[65b] A pervaporation dehydration experiment was carried out utilizing ethanol/water solutions to study the selectivity of these composite materials towards permeation of water. Due to the presence of GO structural defects, nanosheet edge-to-edge slits, and interfacial free volume cavities, channels with high selectivity and transport rate toward water molecules were constructed. The interplay between crystallinity of the polymer matrix and permselectivity of water channels endows the hybrid membrane with enhanced separation performances, and a remarkable long-term operation stability.

2DMs nanosized membranes can be also manufactured by combining diverse coating techniques, *e.g.* drop casting followed by spin coating of a 2DMs dispersion onto the same support surface.[60a] Nair *et al.* reported on the first submicrometer-thick graphene oxide based laminated membranes obtained by spray coating and spin coating, with the ability of almost fully retained liquid, vapor and gas (including helium), allowing at the same time the unimpeded permeation of water **(Figure 4a)**.[64] Scanning electron microscopy (SEM) image show that the obtained films have a very well defined layered structure (**Figure 4b**). Water moleucles can easily pass through capillaries formed by the assembly of graphene oxide layered stacks (**Figure 4c**), while the diffusion of other species (organic solvents, gases) is impeded by the reversible narrowing of the channels in low humidity conditions and by their blocking with H_2O molecules. In general, films obtained using spray coating may not possess homogeneous structure, because of the effect of gravity draining. In this situation the rotation of substrates during spraying may overcome this issue, and it can also represent a suitable method to coat tubular-shaped membranes.[60a] Despite of some well-known advantages, the use of spray coating method in membrane surface modification with 2DMs is still in its embryonal stage.

Thanks to the unique structure of ultrathin layered materials, the typical strategy to easily assemble 2DMs laminar membranes is a filtration process.[15a, 18a, 66] The solvent flows in the limited space offered by the filtration support causing additional interactions between the 2DMs, such as hydrogen bonding, electrostatic and van der Waals interactions, which are responsible for their continous assembly into ordered laminar structures. The thickness and interlayer distance of the laminates, typically in the range or few nanometers to tens of micrometers, can be controlled by using different concentrations of 2DMs. Noteworthy, other functional constituents, such as polymers and other molecular species can be simply integrated with 2DMs, and used to control the interlayer structure of the final laminated hybrid membrane. Dikin *et al.* first reported on the preparation of GO membranes by flow directed assembly of indyvidual GO sheets.[66a] The interlayer spacing resulted to be about 0.83 nm, as inferred by XRD measurements, which is in accordance with the presence of approximately one mono-layer of water in between the GO sheets. Han *et al.* fabricated a ultrathin (22-53 nm) graphene membrane with 2D nanochannels by filtering chemically converted graphene onto a microporous substrate (PVDF and mixed cellulose ester membranes).[15a] The resultant membrane showed an excellent retention performance with a relatively high water flux (21.8 L m^{-2} h^{-1} bar^{-1}), based on the mechanism of physical sieving and electrostatic interaction. Guan *et al.* incorporated 3D zirconium based nanoporous metal-organic frameworks (UiO-66) crystals into a 2D graphene laminated structure, for water desalination based on size-selective diffusion.[67] The 3D/2D membrane exhibited 15 times higher water permeability with respect to reduced graphene oxide membranes produced by hydrothermal reduction of GO in the presence of $NH_{3(aq)}$ and L-ascorbic acid, with similar high retention rate. Chen *et al.* fabricated rGO-CNTs hybrid membranes by intercalation of reduced graphene oxide with carbon nanotubes, using a vacuum-assisted filtration method.[68] The optimized rGO-CNTs hybrid was proposed as a membrane for retaining dyes, sugars, proteins and nanoparticles from water. Experimental results showed high retention efficiencies above 99% (excluding methyl orange),

excellent antifouling properties and good permeability values of 20-30 L m^{-2} h^{-1} bar^{-1}. As a widespread, high throughput method for membranes fabrication, filtration process can be easily extended to other 2D materials, such as MoS_2,[69] WS_2[70] and MXenes, the only limitation being represented by the chemical compatibility between the filter and the solvent in which 2DMs are dispersed, as well as through pore charcateristics.

A method commonly employed for the preparation of thin polymer films, which can also be extended to the preparation of layered stacked membranes, is interfacial polymerization (IP).[71] This process consists in a *in situ* interface reaction between two reactive monomers dissolved in immiscible solvents to form an ultra-thin dense polymeric film (from few nm to several μm thick) at the interface (**Figure 5a**). IP was developed by Cadotte *et al.*[72] and has been used for producing membranes for nanofiltration and reverse osmosis processes.[73] This represented the first example in the literature for a non-cellulosic membrane material with equivalent water flux and salt rejection for monovalent metal ions. The structural morphology and composition of membranes prepared by IP can be controlled by various factors, such as concentrations of monomers, solvent type, reaction's kinetics.[71c, 74] To date, 2DMs sheets have been rarely employed for the realization of hybrid membranes *via* the interfacial polimerization method. For example, Yin *et al.* prepared GO-polyamide nanocomposite membranes for water purification.[75] Their results indicated that by increasing the concentration of GO from 0 to 0.015 wt.% in the 1,3,5 benzenetricarbonyl trichloride (TMC)-hexane phase during the fabrication, the permeate flux under 300 psi increased from ~40 to ~60 L m^{-2} h^{-1} bar^{-1}, while rejections of NaCl and Na_2SO_4 only marginally diminished of around 2%. Recently, Bano and co-workers designed novel nanofiltration hybrid membranes prepared *via* IP, using GO nanosheets incorporated in a polyamide matrix.[76] The results revealed that the addition of GO has a strongly positive impact on both water flux and antifouling properties, with no detrimental side effect on salt rejection. Despite the continuous improvement in the design of thin polymeric

membranes by IP some technical challenges still hamper the use of 2DMs in this field, especially regarding the structural integrity of the resulting hybrid film and the minimization of 2DMs sheets aggregation during the polymerization reaction.

Layer-by-layer (LbL) assembly represents another classical method for the fabrication of layered composite films by means of alternated deposition of oppositely charged species (classically polycations and polyanions), resulting in the growth of ordered stuctures along the substrate's normal direction (**Figure 5b**).[77] The LbL assembly of 2DMs gives the possibility of generating functionalized membranes with excellent separation performance and controlable thicknesses by selecting the number of deposition cycles.[78] Moreover, the interlayer distance can be tuned by chemically modifying the 2DMs, either by covalent or non-covalent approaches, which improves the stability of functional multilayers. Choi *et al.* showed that the coating of multilayered GO with polyamide (PA) thin films *via* LbL approach resulted in a hybrid membrane with improved antifouling properties (due to the hydrophylic protecting PA layer) and resistance to chlorine induced degradation, while maintaining high levels of salt rejection.[79] Interestingly, the water flux through the GO-PA membrane is not affected by the presence of the multilayered GO structure and it is comparable to that of pristine PA membranes (14 L m^{-2} h^{-1}). A similar approach to assemble graphene and 2DMs sheets into laminar membranes is the Langmuir-Blodgett method, which offers the possibility of controlling in plane interactions of materials assembled at the water-air or water-solvent interface by modification of the surface pressure, thus allowing for the formation of monolayers that are eventually transferred on solid substrates.[80] Hu *et al.* covalently cross linked GO sheets with TMC and immobilized them on a polydopamine-coated polysulfone substrate *via* LbL approach.[81] The obtained GO membrane has a free interlayer spacing of approximately 1 nm and a total thickness of approximately 5–50 GO layers, showing high rejection of cationic dyes (Rhodamine B) and water flux of 27.6 L m^{-2} h^{-1} bar^{-1} which is much higher than commercially

available nanofiltration membranes. The same group reported on the alternate layer by layer assembly of GO sheets with poly(allylamine hydrochloride) on a porous poly(acrylonitrile) substrate to fabricate a novel type of water purification layered membranes.[82] The obtained hybrid membranes retained a high structural stability in solutions with low ionic strength, and exhibited high rejection (up to 99%) for sucrose (used as a representative uncharged species). However, the contact of the membrane in solutions with high ionic strength (*i.e.*, $MgCl_2$ 1 M) results in the increase of the interlayer spacing due to the shielding of electrostatic interactions holding the GO and polymer layers together, suggesting that stronger interlayer forces are needed to obtain more stable multilayers.

The final method of hybrid membranes fabrication is the electrospinning.[44] Electrospinning is a special type of the electrospray process in which external high voltage is used to consistently produce fibers with sub-micrometric diameter of numerous organic polymers.[83] A general electrospinning set-up consists of a high voltage (kV) power supply, a syringe connected to a pump and a grounded conductive collector. As soon as the first liquid drops are ejected from the syringe, Coulomb forces originating from the strong electric field between the needle tip and the collector overcome the liquid's surface tension, deforming the meniscus into a conically shaped structure (the so-called Taylor cone) and producing a stream of material that comes out from the nozzle. Finally, as the solvent evaporates and the jet dries, the spontaneous whipping motion of the polymer fiber results in the formation of a non-woven fibrous mat on the grounded collector surface. This simple and effective process capable of generating nanofibers was first described by Zeleny in 1914[84] and patented by Formhals in 1934.[85] Hitherto, various types of polymers have been investigated to obtain electrospun membranes, including polystyrene,[86] poliacrylonitryle,[87] polyvinylidene fluoride (PVDF),[88] chitosan[89] and cellulose acetate.[90] The morphologies of the resulting membranes can be effectively tuned by different parameters such as polymers solution's flow and applied voltage.[91] In general, high porosity and high

specific surface area make electrospun membranes very appealing materials for water purification processes.[92] Feng *et al.* reported on the use of polyvinylidene fluoride nanofibrous membrane, produced by electrospinning, to remove salt from seawater.[93] The membrane could be used in air-gap distillation process to produce water with small salinity (less than 280 ppm) starting from 6 %wt NaCl solution. The electrospinning method has been also applied to the fabrication of 2DMs based membranes. Ren *et al.* assembled sheets of $Ti_3C_2T_x$ into supported membranes for the selective sieving of metal ions and dyes from wastewater.[94] Those MXene membranes presented a micrometric thickness (from 9 to 15 μm) and ultrafast water flux as high as 37.4 L $atm^{-1}h^{-1}$ m^{-2}). In another work, Wang and co-workers obtained multi layers GO membrane surface-overlaid on the electrospun polyacrylonitrile nanofibers for highly efficient removal of pollutants from water.[95] Noteworthy, the prepared bilayer membranes were stable and free of delamination even after the thermal reduction of GO sheets. Najafabadi *et al*. used chitosan/GO nanofibers as a high-performance adsorbent for heavy metal ions from aqueous solutions.[89] The authors used an applied voltage of 20 kV, with a nozzle-collector distance of 15 cm to obtain the hybrid chitosan/GO membranes and were able to effectively adsorb Pb^{2+}, Cu^{2+} and Cr^{6+} metal ions.

In this section, we have outlined some of the currently available technologies for 2DMs-based membranes in terms of their basic components, used methodology, structural features and properties. All the above-mentioned examples of 2DMs are summarized in **Table 1**.

2.2 Transport mechanism

As a result of an emergence of new strategies for inter-particle channel modifications and extended lateral dimensions, 2DMs-based membranes are being considered as a novel platform for effective separation technologies, remarkably facilitating water, gas, and ion transport. The ultra-fast and highly selective transport has been investigated for a long time, but a unifying

picture of the overall mechanism is yet to be reached. Generally speaking, depending on the considered length scale of the membrane pore size, a variety of selective transport mechanisms can be achieved (**Figure 6**).

One among the most interesting and useful working mechanism taking place at the smallest length scale, concerning for instance polymeric and 2DMs membranes used in reverse osmosis and gas separation membranes, is the solution-diffusion mechanism.[96] Diffusion is defined as a spontaneous spread and penetration of species (molecules) from a region with higher chemical potential to another one with a lower chemical potential.[97] The difference in chemical potential may results from a concentration, temperature or pressure gradient. The process in which molecules exhibiting size larger than a membrane pore size are blocked in a membrane due to steric hindrance is called molecular sieving.[98] Besides the molecular trapping, this process can be driven *via* additional electrostatic or chemical interactions with the membrane's surface. At larger length-scale (*i.e.*, sub-μm range), the transport is regulated by Knudsen diffusion for which species with lower molecular mass have higher permeance and travel faster.[18b] Poiseuille flow (also called convective flow) is the pressure-induced pore flow model generally adopted to describe the transport in a capillary or a porous medium.[99] In Poiseuille flow when the pores are very small and the mean free path of the gases and ions is larger than the pore diameter, collisions with the pore will occur and the lighter molecules will then preferentially pass through the membrane.

In general, transport through membrane pores with size larger than molecules or ions results to be affected by electrostatic interactions, steric effects and chemical affinity.[100] Diffusion mechanism is considered as a key process for harvesting *blue energy* using membrane separation of molecular species – ions from water in PRO and cations from anions in RED. Nevertheless, some reports have presented that molecular separation in PRO and RED are not mandatory for osmotic flow. Diffusio-osmotic transport was introduced by Derjaguin in the

1940s and it has been overlooked for many years, until some recent works brought it back under the spotlight.[101] Diffusion-osmosis transport is a surface mechanism driven by an osmotic pressure gradient occuring within few nanometres from the surface of the membrane pores (**Figure 7**). In this case, the use of semipermeable membranes is not necessary, because the osmotic flow would result from specific interactions between the solute (in this case, a salt) and the surface. The difference in ionic concentration produces an electric current, known as the diffusion-osmotic current, as the ions move across the membrane subjected to the interfacial osmotic pressure gradient. Diffusion-osmosis is therefore a halfway process between PRO and RED, and since it occurs at the surface, increasing the surface area of the membranes translates in a higher ionic current. This mechanism has been exploited in membranes made of 2DMs and has been shown to provide particularly efficient osmotic power conversion. Further discussion about "anomalous" transport mechanisms associated with phenomena occurring within the membrane in the nano and sub-nano scale regime[29b, 102] and originating from the interaction of the ions with the surface of the nanopores at the Debye layer (λ_D) length scale is presented in **section 3.2.1**.

Despite the fact that the transport of chemical species through a membrane is a complex process and is still the subject of fundamental investigations, an atom thick selective layer endowed with precisely controlled porosity and chemical functionality based on 2DMs is unquestionably advantageous for achieving high permeation and selectivity. Therefore, further investigations aiming at achieving a full control over membranes nanostructuration and over the mass transport in atom thick porous materials, would lead to more and more effective solutions for seawater desalination and osmotic energy harvesting, as well as gas separation and catalysis.

3. 2DMs in reverse electrodialysis (RED) and pressure retarded osmosis (PRO) processes

RED and PRO are emerging membrane-based technologies that enable converting chemical energy of salinity gradients in useful work. RED and PRO have inherently different working mechanisms. RED is based on a charge-driven flow provided by ions passing through a stack of ion exchange membranes generating a chemical potential difference. PRO is based on water permeation through a semipermeable membrane as a consequence of the concentration gradient between draw and feed solutions, with $C_{draw} > C_{feed}$. The volume expansion of the more concentrated solution resulting from the permeation of water in the draw reservoir causes a pressure build-up, that is partially released by an outlet flow powering a hydroturbine. Both RED and PRO rely on partial transport through a semi-permeable membrane, with the flow of water scaling inversely with the membrane's thickness. 2DMs exhibit multiple crucial features, including chemical inertia and high adsorption selectivity towards different chemical species, making them exceptionally suitable for membranes fabrication. Moreover, 2DMs exhibit extreme mechanical strength allowing for application of high external pressures, which are required in both RED and PRO applications. As the pores size significantly influences permeation of specific molecules through the membrane, creating pores in a controlled fashion is key for any membrane-based processes. Therefore, tunable thickness and the ability to introduce various defects, including sub-nanometer sized pores, over a large surface area make 2DMs ideal materials for their use in *blue energy* generation. Porous graphene, for example, constitutes a particularly attractive candidate for applications in desalination, nanofiltration and other membrane-based processes.[103] Notably, several approaches can be followed to prepare micro- and mesoporous graphene, as well as other 2DMs. In Section 2 we have described in detail some of the recent and most promising *top-down* fabrication techniques used to obtain porous 2DMs, also highlighting some of the critical drawbacks (*e.g.*, poor scalability of electron-beam fabrication, poor control of pore size distribution for oxidative methods). Noteworthy, semi-permeability is a crucial characteristic of membranes for pressure retarded osmosis, as the water needs to flow across the membrane with the highest flux possible. On the

other hand, reverse electrodialysis is mostly based on ion-exchange membranes, therefore their physical and electrochemical properties should be taken more into consideration. In this regard, as 2DMs can provide multiple functionalization pathways, anion and cation exchange membranes (AEM and CEM, respectively) based on 2DMs can benefit from additional chemical modification aimed at higher permeate selectivity and increased ionic current.

3.1 Reverse Electrodialysis (RED)

In RED process brine and a freshwater are let passing through a stack of alternating anion and cation exchange membranes (AEM and CEM, respectively) generating adjacent highly concentrated (HC) and low concentrated (LC) compartments. The salinity gradient induces a chemical potential difference over each membrane's side with a corresponding flux of water molecules from the LC compartment to the HC compartment (**Figure 8a**). However, due to the presence of ion exchange membranes, only counterions can selectively permeate through each LC compartment and the difference in ion concentration across both AEM and CEM produces an electrochemical potential difference. The total electromotive force generated in RED, *i.e.* the open circuit voltage (OCV), is the sum of the Nernst potential over each cell. For relatively diluted NaCl solutions and 2 ion exchange membranes:[104]

$$OCV \sim \frac{2\alpha RT}{zF} ln\left(\frac{c_{HC}}{c_{LC}}\right) \quad (4)$$

In which α is the membranes permselectivity, z is the valence of the exchanged ions, T is the temperature, F is the Faraday constant, R is the Boltzmann constant and c_{HC} and c_{LC} are the concentration of the HC and LC compartments, respectively. The resulting ionic flux is then transformed into an electric current at the end electrodes with a suitable reversible redox couple, and electric work is produced by using an external load resistance.[104-105]

RED operating mechanism can be described according to Nernst-Planck transport theory with a few important factors having significant influence on the overall performance, namely membrane thickness, water transport and co-ion transports through the membranes.[106] Theoretical and experimental results show that membrane thickness plays a remarkable role in current efficiency and effective performance in RED. Investigations on membranes with thickness in the range of 10-100 μm performed by Tedesco *et al*. revealed that thinner membranes are able to produce higher power density, as long as they remain structurally stable and highly selective.[106a] Membrane's selectivity indeed represents, at least from a materials science perspective, the predominant feature for reverse electrodialysis, since the effect of co-ion transport through the membrane may reduce the density power of about 20%.[106c] Other factors affecting RED performance and practically limiting *blue energy* harvesting are schematically displayed in **Figure 8b**. The useful work produced in RED is indicated by the black patterned area, entropy production due to resistive energy loss caused by internal resistance of the RED stack is depicted in blue, while the resistive loss associated to uncontrolled mixing, *i.e.* water and co-ions leakage, is marked in red. The area depicted in green indicate the amount of energy unutilized because of premature discontinuation of the process.[104-105]

One among the challenges for effective energy production from reverse electrodialysis is the design and fabrication of appropriate membranes with ion/molecules selective nanochannels. Typically, smart nanochannels can be obtained using defect-rich functional materials, by self-assembly processes and ion-track-etching or electrochemical etching.[75, 107] Since RED practically requires a series of ion exchange membrane pairs in order to provide effective electrochemical potential, the application of ultrathin membranes with low resistance is necessary (**Figure 9a**).[104, 108] It is estimated that the maximum amount of salinity gradient energy that can be harvested from 1m^3 of freshwater and 1m^3 of sea water is about 1.8 MJ.[109]

Notably, the amount that can be harvested with RED strictly depends on the energy efficiency of the process.[110] Two different approaches might be distinguished in terms of application of two-dimensional materials in reverse electrodialysis. The first is based on the preparation of selective membrane (CEM/AEM) providing ion migration and chemical potential generation. On the other hand, since 2DMs exhibit unique electrical properties, they can also be utilized as electrode materials.[111]

Wan *et al*. have presented porous graphene with controllable pore size as a potential material for RED.[112] The porous graphene was obtained with a microwave combustion process of a GO – metal precursor mixture (*e.g.*, silver acetate, cobalt nitrate, ammonium molybdate, copper nitrate) and subsequent washing of the formed NPs. Then, the obtained porous graphene was placed together with an anodic aluminum oxide (AAO) membrane (with pores size around 60 nm) between two gaskets (**Figure 9a-b**) and the so-obtained asymmetric ion-selective membrane with pore size of 5, 30 and 100 nm was investigated towards salinity gradient power generation. The sample with the smallest pores exhibited the best power density, equal to 1.15 W m^{-2} as tested in 1 M - 10^{-6} M NaCl set. To the best of our knowledge, this membrane shows the highest power density among graphene-based RED devices.

Another approach was recently proposed by He *et al*. and relies on a use of graphene hydrogel as an electrode for RED process.[113] The electrode material was prepared by using a one-step hydrothermal reduction, followed by the soaking of the obtained hydrogel in hexadecyl trimethylammonium bromide and subsequent compression to form tablets. A RED cell was prepared by assembling commercially available filtration and anion-exchange membranes between a high-concentrated (500 mM NaCl) and low-concentrated (20 mM NaCl) solutions, with the open circuit potential measured using the Ag/AgCl electrode. The proposed RED set exhibited a power density of 482.4 mW m^{-2} when an anion exchange membrane was used. Rollings *et al*. reported on a graphene membrane with high ion selectivity.[114] Nanopores

generated *via* electrical pulse method enabled selective permeability of potassium ions. Experiments were performed in different KCl solutions using Ag/AgCl electrode. The obtained material exhibits promising results for cation exchange membrane with high potential for RED application.

TMDs are also being investigated as membrane materials for RED. In Section 2 we already discussed the use of a single-layer MoS_2 with a single nanopore proposed as an osmotic nanopower generator.[29b] Based on the membrane efficiency, it was extrapolated that the osmotically induced current reached 10^6 W m^{-2}, which is approximately three orders of magnitude greater than the value obtained with boron nitride nanotubes,[55] and six orders of magnitude higher than the power density obtained in RED with classical membranes (*e.g.*, cellulose acetate or polyamide membranes).[9] A more practical application of TMDs in reverse electrodialysis was presented by Jeong *et al*. who utilized MoS_2 and a hybrid of MoS_2 and porous carbon to prepare a very efficient cathode material. The porous carbon substrates were directly coated *via* CVD process by heating $Mo(CO)_6$ and S_2 under inert gas conditions. The RED tests were performed on fifty pairs of ion exchange membranes for 0.5 M - 1 M NaCl solutions using Ti-mesh supported Pt as an anode. The investigated hybrid system exhibited a maximal power density of around 0.48 W m^{-2}, which is more than double to that of a pristine MoS_2 electrode (0.2 W m^{-2}).

Table 2 summarizes all the above-mentioned examples of 2DMs-based membranes and electrodes used in reverse electrodialysis.

3.1.2 Ionic diodes and RED systems exploiting ionic transport in nano-sized channels

Similar to a diode in electronics, an ionic diode can be defined as a device with the property of asymmetric electric conductance in which ions preferentially flow in one direction.[115] While in Nature asymmetric ion channels allow ionic transport in one direction to perform complex biological functions,[116] the presence of nano-sized channels with rectified ionic transport

within a membrane can be particularly beneficial for RED-based processes thanks to enhanced selectivity. The charge selectivity in such devices derives from peculiar transport mechanisms occurring when the size of the channels connecting water solutions reservoirs approaches the dimensions of the hydration layers formed around each ion (*i.e.*, Debye length). A different concentration profile of counter-ions and co-ions can be due, for instance, to Coulomb interactions between ions and charged channel walls. In this regime, the ion conductance through the nanochannel is ruled by the surface charge instead of the ion concentration in the reservoir.[117] This ionic diode behavior can also be observed when other symmetry breaking factors occur, namely asymmetric shape of the channel (*e.g.*, conical-, funnel, bullet-shaped nanochannels),[115] partial charging of the nanochannel surface[118] and concentration gradient across the nanochannel.[119] The working principles of ionic diodes are based on ions flow promoted by pressure gradient in the channel. This phenomenon induces counter ions flow in the double layer at the channel walls leading to generation of electrical current. In details, as the inner surface of the channel is charged, the advection of ions creates streaming potential resulting in electro-kinetic energy conversion from mechanical to electrical (**Figure 10a**). Moreover, nanofluidic systems make it possible to determine the highest energy conversion efficiency by probing of the regime of double layer overlap.[120] Therefore, porous materials with high specific surface area with potential to induce p-n junction constitute attractive materials for such systems for harvesting *blue energy*.[121] Ion transport through nanochannels can be compared to electrons and holes in semiconducting nanomaterials or Shockley diodes.[101a, 122] The current generated during the process can be expressed by the Shockley equation:[123]

$$I = I_S\left(exp\left[\frac{eV}{k_BT}\right] - 1\right) \quad (5)$$

where I represents the ionic diode current, I_S is the so-called saturation current, e is elementary charge, V is the voltage and T is the temperature.

Nanofluidic RED-based energy harvesting systems have been recently investigated and they have shown high power densities and energy conversion efficiencies. Long *et al.*[124], for instance, have performed numerical simulations to illustrate the electrokinetic behavior of asymmetric nano-sized channels (R_1=5 nm, R_2= 10 nm) connecting NaCl reservoirs of different concentration. Their results show that due to the asymmetric geometry of the bilayer channel, the performance of the nano-fluidic RED is strongly impacted by the direction of the applied NaCl concentration gradient because of the different degree of electric double layer overlap in the selected asymmetric configuration. Hwang *et al.*[125] used a thin mesoporous silica membrane with uniaxially aligned pores (thickness ~55 nm, pore size = 2-3 nm) to separate reservoirs of monovalent electrolytes of different concentration. Interestingly, the power density of their devices shows a cation-specific dependency (3.90 W m^{-2} for KCl, 2.39 W m^{-2} for NaCl, 1.29 W m^{-2} for LiCl) suggesting that a larger difference in the diffusion coefficient of ions and cations, leads to a higher power density. An ionic diode membrane with asymmetric structure, chemical composition and surface charge polarity has been developed by Gao et al.[126] by employing a mesoporous carbon (pore size ~7 nm, negatively charged) - microporous alumina (pore size ~80 nm, positively charged) heterojunction. The peculiar design of the membrane lead to rectified ion transport through the meso/macro channels with high selectivity, even in highly concentrated electrolyte solutions. When artificial seawater and river water are mixed through the ionic diode membrane, a remarkable power density of up to 3.46 Wm^{-2} is obtained. Another noteworthy experimental work that highlights the role of the channel size in nanofluidic devices was presented by Esfandiar *et al*. who investigated ion transport through angstrom-scale slits.[127] Their devices were constructed by assembling different crystals (graphene, hexagonal boron nitride, MoS_2) on top of bilayer graphene and MoS_2, which served

as spacers, resulting in a stacked membrane with channels height of ~0.7 Å. By performing conductivity tests with KCl solutions permeating these slits, a deviation from linearity of the conductance around 10^{-2} M was observed (**Figure 10b**) and slight dependence on the composition of the channels walls, apart from higher saturation values of the conductance that were ascribed to variable surface charges of the channels' walls (**Figure 10c**). Interestingly, large ions (*i.e.*, hydrodynamic diameter larger than 13 Å) are completely excluded from the Å-scale channel, while ions with hydrated diameters slightly larger than the slit size permeate with reduced mobility, presumably upon distortion of their hydration shells. The confinement effect also translates in a remarkable asymmetric transport between anions and cations of the same diameter (*i.e.,* anions generally show reduced mobility), which is explained by considering the different orientation of water molecules in their hydration shell and the polarization effect exerted by the channel's surface. The presented results emphasize the importance of 2DMs to develop nanofluidic systems with size- and/or charge-selective transport and might build the foundations for next-generation RED systems.

2DMs-based membranes endowed with nanofluidic channels have been recently proposed as potential candidates for high-performance ion-exchange and electro-dialysis technologies, due to their nonlinear ionic transport. For example, Hong *et al.*[128] have measured the ionic permeability of a GO membrane (thickness = 3 μm) fixed on a porous substrate separating two compartments filled with electrolyte solutions and electrically contacted with Ag/AgCl electrodes (**Figure 11a**). The GO membrane showed high cation selectivity for different salts (monovalent cations > bivalent cations > trivalent cations) due to the negatively charged surface of the membrane's nanochannels (*i.e.*, oxygen-carrying functional groups). The ion-rejection in GO membranes results to be determined as much by the electro-static repulsion (*i.e.*, nanochannel surface charge) as it is by the size-exclusion effect (*i.e.*, nanochannel height).

Hence, surface modification of GO nanosheets may offer a new route for increasing the overall salt rejection, without lowering the water flow across the membrane.

An interesting approach was presented by Ji *et al*. by using GO-based charged nanofluidic membrane (GOM) pairs (interlayer distance ~1 nm, thickness = 0.5 – 100 μm).[121a] Pristine graphene oxide was used as a cation exchange membrane (*i.e.*, negatively charged membrane), while a carbodiimide-mediated ligation is employed to conjugate positively charged 1-aminopropyl-3-methylimidazolium bromide onto GO surface, reverting its charge and making it the anion exchange counterpart (**Figure 11b**). These charged GOM stacked pairs showed surface charge-governed transport and were able to generate high voltage (up to 2.7 V), as well as to provide a power density as high as 0.77 W m^{-2} when tested in a 0.5 M - 0.01 M draw-feed NaCl solution set.

A dramatic reduction of the nanochannel size could also lead to the emergence of quantum-like ionic transport, as demonstrated by Feng *et al.* who separated two ionic solutions with a single-layer MoS_2 membrane featuring a single 0.6-nm-diameter nanopore, biased by a pair of Ag/AgCl electrodes (**Figure 11c**).[129] Pronounced non-linear I-V characteristics are observed, with the current being suppressed at small voltages, and increasing more strongly when the bias voltage exceeds a threshold value (apparent gap ~400 mV). All the tested chloride salts (K^+, Na^+, Li^+, Ca^{2+}, Mg^{2+}) exhibited nonlinearity, with different voltage gaps for different ions and a strong dependence on the cation's valence. The observed phenomenon differs drastically from traditional ion transport through larger nano-sized pores, with the suppressed conductance in the subthreshold regime being attributed to the finite energy barrier to overcome in order to add a charge carrier to the pore, and to the stepwise free energy barrier required to break ion's hydration shells when it permeates through pores smaller than 0.8 nm. Another relevant example of anomalous ionic transport occurring at Å-scale length is that reported by Motuerde *et al.*[130] In their work the authors were able to study the purely two-dimensional flow of water

and ions through Å-scale channels realized by van der Waals assembly of 2D crystals of graphite (or hexagonal boron nitride) and by-layer graphene spacers on a SiN membrane, separating two reservoirs filled with KCl solutions and containing Ag/AgCl electrodes. Each device had channels with height ≈ 6.8 Å, width = 130 nm and length of a few micrometers (**Figure 11d**). The ionic transport, propelled by pressure and by an applied electric field, revealed a highly nonlinear transistor-like electrohydrodynamic effect. The application of a small voltage is able to "switch" the ionic transport (characterized by streaming mobilities), and such gating effect results to be markedly dependent on channel material's composition. The authors described the system's behavior with an extended Poisson–Nernst–Planck model and attributed the bias-dependent high streaming mobility to the unusually fast transport of water and hydrated ions at molecular distances from the channel surfaces.

Considering the aforementioned examples and the fast, continuous progress in nanomaterials manufacturing technologies, further engineering of materials at the nano-scale aimed at the full control of the ionic transport mechanism in atomically thin, small and ultra-small (<1 nm) pores, will definitely result in the development of highly selective next-generation membranes, and likely stimulate fundamental research in novel domains of physical chemistry, nanoscale fluidics and biology.

3.3 Pressure Retarded Osmosis (PRO)

Osmotic energy represents a sustainable solution for the production of energy, with high potential and a significantly lower amount of pollutants created during the process. Pressure Retarded Osmosis (PRO) has become an attractive method for power generation by means of osmotic energy and it is based on the application of a semipermeable membrane separating two modules with a high salinity gradient. In order to equilibrate the chemical potential of the two solutions (see Chapter 1), water flows from the low-concentrated feed solution to the high-

concentrated draw solution. As a consequence, an elevated pressure – up to approximately half of the difference in osmotic pressures between the two solutions – builds-up on the side of the membrane facing the draw solution, increasing the flow and simultaneously powering an outlet turbine that generates electricity. An actual PRO system consists of membrane modules in continuous flow operation, *i.e.*, water solutions advance along the axial length of the membranes in direct current configuration **(Figure 12a)**. **Figure 12b** shows a schematic representation of a PRO system, in which the osmotic flow of water from the LC to the HC compartment produces an increase of the volume ΔV and a corresponding excess pressure ΔP. The useful work that can be obtained using PRO can thus be calculated with the following equation[131]:

$$U = \int \Delta P \, dV \tag{6}$$

However, similar to RED, several factors practically lower the amount of energy extractable in PRO (**Figure 12c**), such as frictional loss originating from the permeation of water through the membrane, as well as uncontrolled mixing originating from the diffusion of salt from the HC side to the LC solution due to a non-perfect selectivity of the membrane.[105]

The PRO method constitutes an attractive energy source and gained considerable attention since its invention by Loeb in 1973.[132] Further developments of the technology recently resulted in the first osmotic power plant prototype installed in Norway in 2009. PRO can be effectively used to capture natural salinity gradient directly exploiting natural seawater-river interfaces, however efficient technologies for energy conversion are still required.[9] It is estimated that global energy production potential of PRO exceeds 2 TW, which constitutes about 20% of the current energy consumption worldwide.[11] Therefore, implementation of PRO-based energy harvesting definitely represent a global strategic target. An important parameter to be

considered is power density (W), which can be defined as the osmotic energy output per unit membrane area and can be calculated from[133]

$$W = J_W \Delta P \quad (7)$$

where ΔP represents the trans membrane pressure and J_w represents the water flux. In order to make PRO economically advantageous, it is estimated that the target power density should exceed 5 W m^{-2}.[134] Notably, implementation of PRO requires a few serious challenges to be taken into consideration such as module design, membrane's thickness and anti-fouling properties.[135] Typically, a potential material for building such membranes should provide high water flux, hydrophilicity, good solute retention and high power density. Moreover, the main challenge associated to the practical applicability of PRO in *blue energy* harvesting is the fabrication of low-cost membranes able to develop a low internal concentration polarization (ICP) during operation. Concentration polarization occurring at the membrane-liquid interface is indeed one of the key factors that most dramatically lower the effective osmotic flow and the final power density of the system.[136] Furthermore, in order to avoid complications related to membrane fouling the feed stream requires pre-treatment, resulting in a considerable energy consumption.[137] Since the water transport through the membrane is strictly dependent on membrane thickness, two-dimensional materials have been recently considered as promising alternative providing minimization of transport resistance and ultimate increase of water flux.[15e, 29b, 138] In this regard, the objective would be to achieve a controllable and selective transport through atomically-thin membranes of graphene, graphene oxide, TMDS and their corresponding hybrid materials, which have been recently widely developed for nanofiltration and separation techniques.[20b, 64, 139] Additional functionalization and defect engineering of 2DMs may constitute powerful tool in the development of next generation membranes.

Tong *et al.* reported on the application of a free-standing graphene oxide membrane (GOM) in pressure retarded osmosis.[140] The membrane was fabricated using vacuum filtration method by pouring a graphene oxide dispersion onto inorganic porous AAO filter, resulting in a thin GOM, which was dried, peeled and used as prepared. Several samples with different thickness ranging from 1.73 μm to 4.12 μm were investigated, with the thickest membrane showing a 40-fold decrease in the water permeability coefficient. These GO membranes presented a power density as high as 24.63 W m^{-2} with a water flux of 4.27 L m^{-2} h^{-1} bar^{-1} using NaCl 3 M and NaCl 0.017 M as draw and feed solutions, respectively. To the best of our knowledge, this represents the best performance reported so far for 2DMs-based PRO membranes. Another interesting example is provided by Hu *et al*.[141] In their work, GO was electrostatically attached to a porous poly(acrylonitrile) by employing poly(allylamine hydrochloride) as a support film, resulting in a layer-by-layer assembled membrane with thickness around 80 nm. The prepared membrane was consequently tested using DI water as feed solution and sucrose solution in range of 0.2-0.9 M as draw solution. The GO-based set was tested toward forward osmosis and pressure retarded osmosis exhibiting a water flux as high as 5.8 L m^{-2} h^{-1} atm^{-1}. However, higher porosity and smaller thickness are needed to make such membrane fully applicable.

Another functionalized GO-based nanostrucure was reported by Lim *et al*. by incorporating GO sheets on halloysite nanotubes.[142] The obtained nanocomposite was deposited on a polysulfone substrate and tested using DI water and 1M NaCl as feed and draw solutions, respectively. The presence of GO provided significant reinforcement of the membrane allowing highly pressurized conditions. The presented membrane for pressure retarded osmosis exhibited optimal power density equal to 16.7 W m^{-2} with a water permeability coefficient of 2.31 L m^{-2} h^{-1} bar^{-1}, making it a great candidate for practical use in PRO applications. Despite the amount of practical applications of 2DMs in pressure retarded osmosis is still limited, the ongoing investigation of graphene, TMDs and other atom thick materials towards semipermeable membranes suggests promising results in scaled-up systems for harvesting blue energy.

4. Conclusion and perspective

This Review presented an outline of various techniques used to fabricate atomically-thin membranes with controlled porosity and their application in the field of water purification and salinity gradient energy harvesting. In particular, *blue energy* originating from controlled mixing of solutions with different salinity is an environment-friendly, renewable energy source and, unlike wind or solar energy, can be harvested in continuous exploiting natural aquatic systems (*e.g.*, estuaries) and any brackish/fresh water boundaries. By considering the latest developments in the field, we foresee that this source of energy would soon reach a level where it becomes viable at a large-scale, playing a decisive role in future's global energy supply.

According to their unique physico-chemical properties and transport mechanism, 2DMs-based membranes show immense potential for next-generation separation technologies and efficient *blue energy* harvesting materials. However, their full development into practical and large-scale applications are yet to be achieved. Some of the challenges to be tackled in the near future will be attaining a higher control over porosity and mechanical resistance, further exploiting defective sites in 2DMs and pore edges to insert additional chemical functionalities, as well as realizing ordered *in-plane* and *out-of-plane* assemblies on a larger scale. Among the several available methodologies, defects engineering by electrochemical methods is emerging as one of the most promising options thanks to its low complexity and the ease of industrial scale-up toward mass production. Electrochemical functionalization and the realization of 2D covalent organic frameworks (2D COF) *via* direct chemical functionalization of 2DMs, could further increase the selectivity of the membranes toward specific chemical species, paving the way to the application of 2DMs not only in separation processes but also in sensing and bio-sensing platforms. On the other hand, alongside with CVD fabrication methods and *top-down* surface engineering technologies, liquid-phase exfoliation and brick-and-mortar assemblies of 2DMs have proven to be particularly well suited for the realization of layered stacks and hybrid films,

especially because of the possibility to manufacture membranes on a large-scale and the virtually unlimited number of available materials that can be used as substrates.

The large-scale production of high-quality 2DMs indeed represents a key step towards development of real technologies and commercial applications. In this regard, special efforts have to be devoted in the near future to novel and improved production methods that could be easily integrated with ordinary industrial equipment,[143] and operate in continuous, such as roll-to-roll CVD or roll-to-roll mechanical processing. Thanks to the continous progress of advanced nanofabrication techniques and novel chemical engineering routes, as well as to the tremendous effort of several groups working at the interface between physics, chemisty, materials science and nanotechnology, membrane-based processes, such as PRO and RED, will certainly continue to profit from the development of two-dimensional materials, eventually leading to the emergence of effective technologies for the harvesting of *blue energy* and water purification.

Acknowledgements

This work was supported by the National Science Center (Grant No. 2015/18/E/ST5/00188 and Grant No. 2017/27/N/ST5/00173) and the European Commission through the Graphene Flagship Core 2 project (GA-785219), the Agence Nationale de la Recherche through the Labex project CSC (ANR-10-LABX-0026 CSC) within the Investissement d'Avenir program (ANR-10-120 IDEX-0002-02), and the International Center for Frontier Research in Chemistry (icFRC). The work was also supported by grant no. POWR.03.02.00-00-I026/16 co-financed by the European Union through the European Social Fund under the Operational Program Knowledge Education Development. D.P. acknowledges the support from the Embassy of France in Poland in the form of a scholarship at the Institut de Science et d'Ingenierie Supramoleculaires, University of Strasbourg.

Conflict of interest

The authors declare no conflict of interest.

Received:

Revised:

Published online:

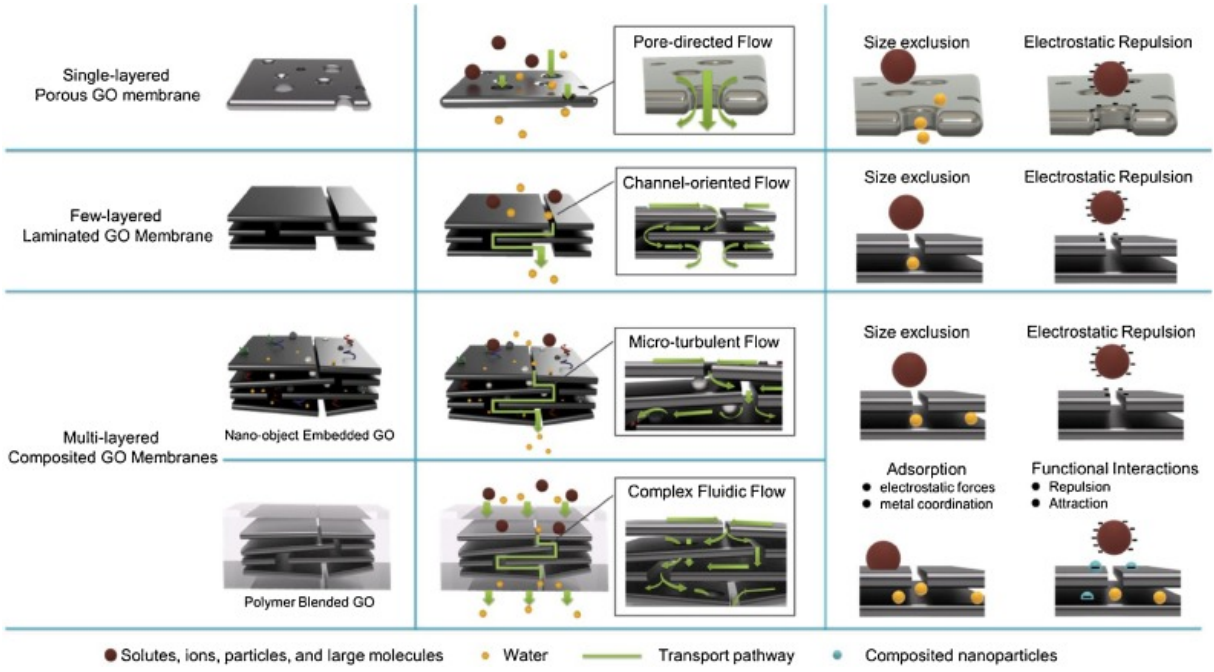

Figure 1. Schematic diagrams summarizing single, few and multi-layered porous GO (taken here as a model 2D material) membranes with their corresponding microfluidic flowforms and structural properties. Reproduced with permission.[144] Copyright 2018, Elsevier Ltd.

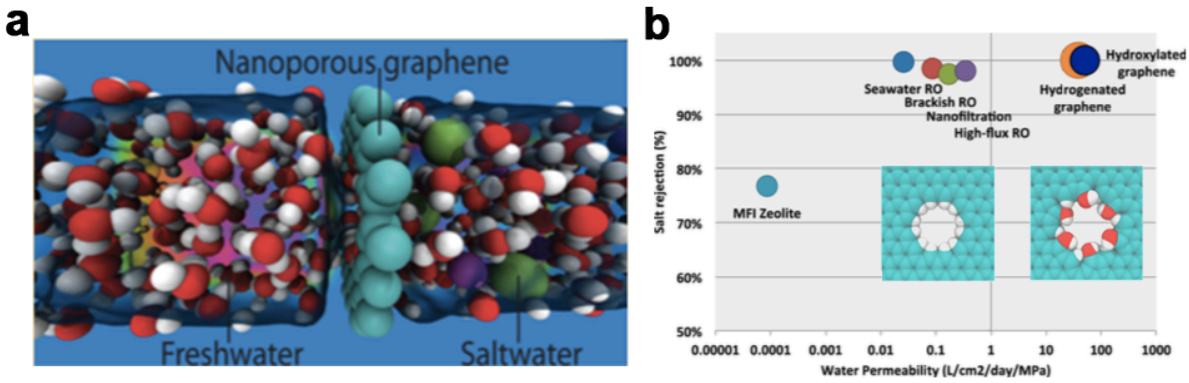

Figure 2. a) Side view of a nanoporous graphene membrane. b) Salt rejection efficiency as a function of water permeability for nanoporous graphene, compared to existing technologies. The inset shows a schematic picture of hydrogenated (right) and hydroxylated (left) graphene nanopores. Reproduced with permission.[15d] Copyright 2012, American Chemical Society.

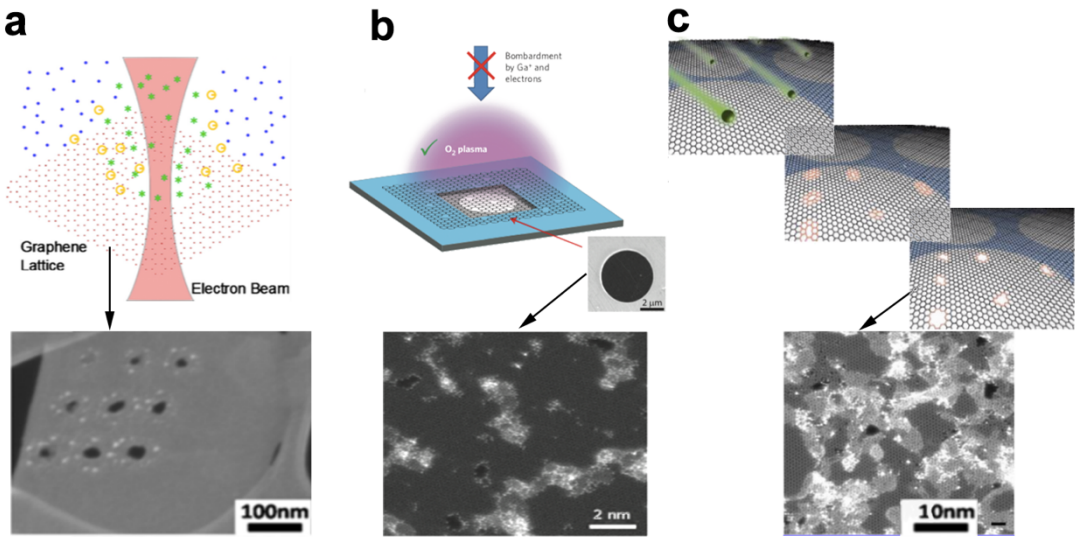

Figure 3. a) Electron beam irradiation and SEM image of nano-pores on a single layer graphene flake. Reproduced with permission.[52] Copyright 2011, American Institute of Physics. b) Schematic image of a porous graphene membrane suspended on a 5 μm diameter hole and STEM image of nanoporous graphene membrane after 1.5 s exposure to oxygen plasma.[19b] Copyright 2014, American Chemical Society. c) Creation of randomly-distributed sub-nanometer pores in a graphene membrane using ion bombardment followed by chemical oxidation. Reproduced with permission.[19a] Copyright 2014, American Chemical Society.

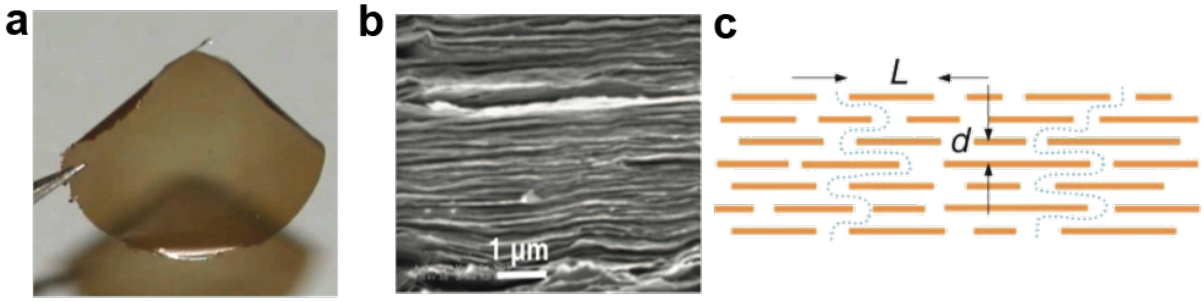

Figure 4. a) Photograph of a 1 mm-thick GO film peeled off from a Cu foil. b) Electron micrograph of the film's cross section. c) Schematic view for possible permeation pathways through the laminates (L/d ~1000). Reproduced with permission.[64] Copyright 2012, American Association for the Advancement of Science.

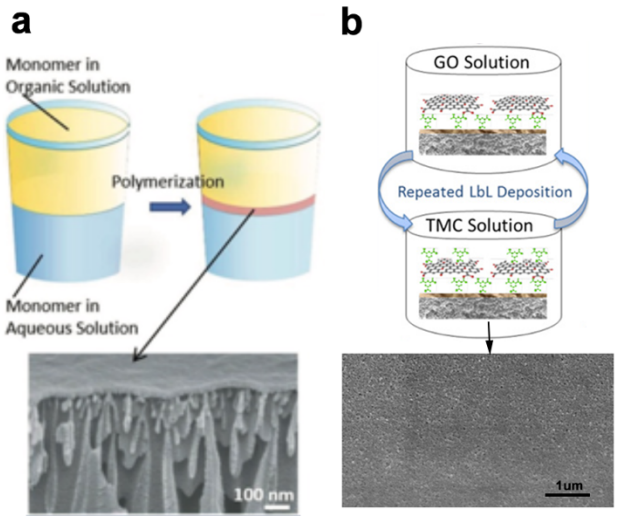

Figure 5. a) Schematic represetation of the interfacial polymerization reaction. Reproduced with permission.[145] Copyright 2016, Springer Nature. b) Schematic ilustration of synthesis GO membrane *via* layer by layer (LbL) assembly. Reproduced with permission.[81] Copyright 2013 Amercian Chemical Society.

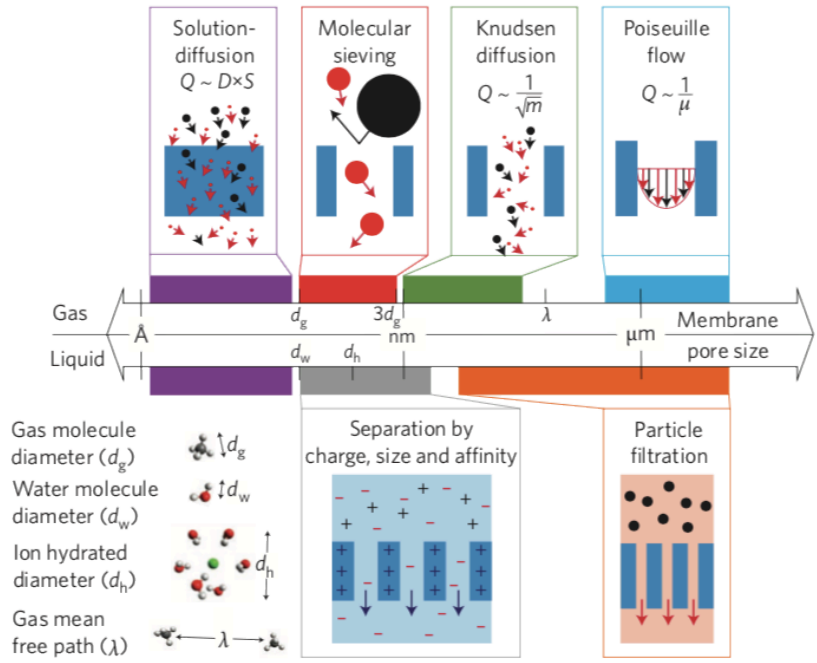

Figure 6. Length scale dependence of membrane transport mechanisms (Q = flux, D = diffusivity, S = sorption coefficient, m = molecular mass, μ = viscosity). Characteristic dimensions of gas and water molecules, hydrated ions and gas mean free path are depicted on bottom left. Reproduced with permission.[16b] Copyright 2018, Elsevier Ltd.

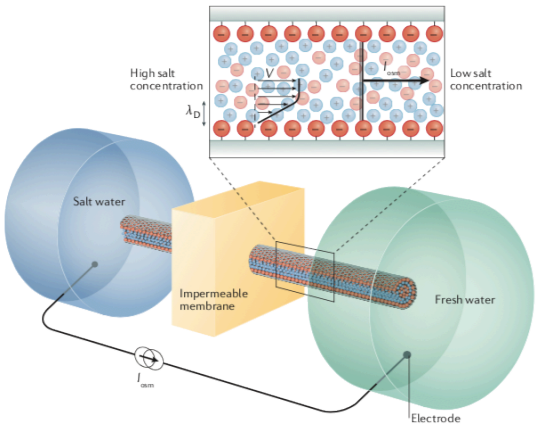

Figure 7. Diffusion-osmotic process for osmotic energy conversion. Reproduced with permission.[17d] Copyright 2017, Springer Nature Publishing AG.

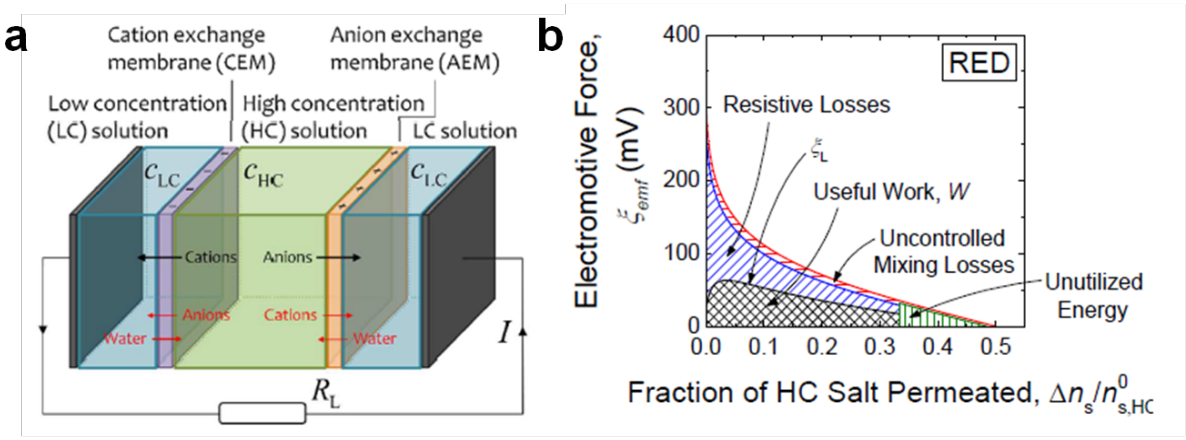

Figure 8. a) Schematic representation of a reverse electrodialysis (RED) cell constituted by two ion exchange membranes. b) Representative plot of useful work (W), fractional/resistive loss, uncontrolled mixing loss and unutilized energy for RED. The horizontal axis denotes the progress of the energy production process, i.e., the fraction of salt permeated from the HC compartment. The presented data refer to NaCl solutions simulating seawater-river interface (HC=0.6 M, LC=1.5 mM) and membrane's properties in accordance with technologically available high-performance ion exchange membranes Reproduced with permission.[104] Copyright 2014, American Chemical Society.

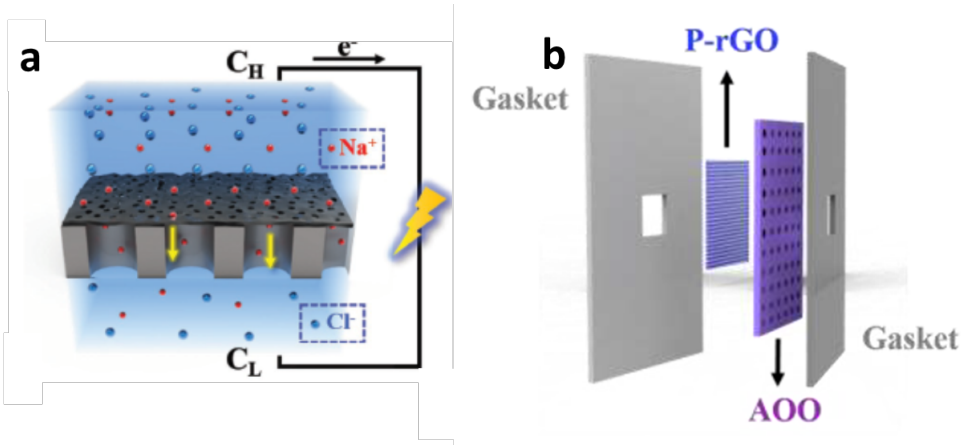

Figure 9. a) Nanoporous rGO ion exchange membrane, and b) experimental set-up for salinity gradient power generation. Reproduced with permission.[112] Copyright 2018, WILEY-VCH.

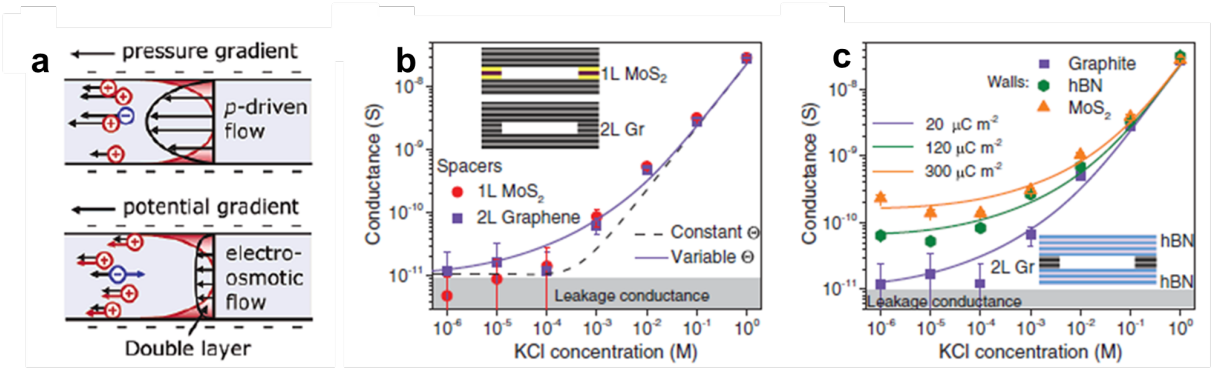

Figure 10. a) Schematic representation of electrokinetic effects. Top: pressure driven- Down: electric field driven energy conversion in nanofluidic channels. Reproduced with permission.[120] Copyright 2006, American Chemical Society. Conductance as a function of KCl concentration for b) devices with 2 layered graphene and MoS_2 used as spacers and c) devices made from graphite, hBN and MoS_2 as upper and bottom walls. Reproduced with permission.[127] Copyright 2019, American Association for the Advancement of Science.

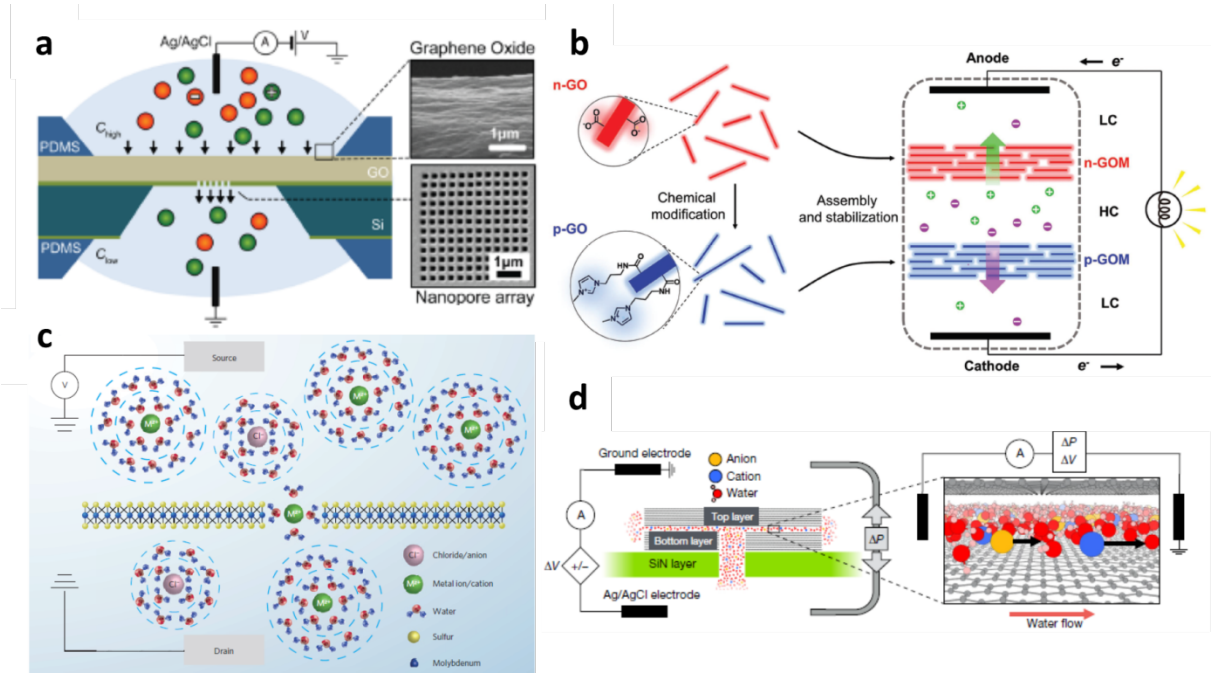

Figure 11. Schematic representation of 2DMs based nanofluidic channels utilizing: a) GO membrane. Reproduced with permission.[128] Copyright 2016, American Chemical Society. b) negatively/positively charged GO. Reproduced with permission.[121a] Copyright 2016, WILEY--VCH. c) porous single-layer MoS_2. Reproduced with permission.[129] Copyright 2016,

Macmillan Publishers Limited. d) graphite/hBN with graphene spacers. Reproduced with permission.[130] Copyright 2019, Springer Nature Publishing AG.

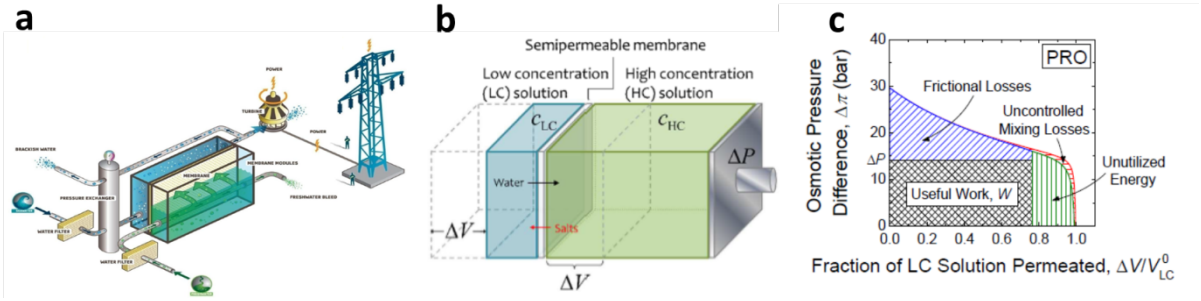

Figure 12. a) Schematic diagram of the pilot PRO plant proposed by Statkraft.[42a] b) Schematic representation of Pressure Retarded Osmosis (PRO) process. c) Representative plot of useful work (W), fractional loses, uncontrolled mixing loses and unutilized energy for PRO. The horizontal axis denotes the progress of the energy production process, i.e., the fraction of salt permeated from the HC compartment. The presented data refer to NaCl solutions simulating seawater-river interface (HC = 0.6 M, LC = 1.5 mM) and membrane's properties in accordance with technologically available high performance ion exchange membranes Reproduced with permission.[104] Copyright 2014, American Chemical Society.

Table 1. Examples of 2D materials-based porous membranes, layered stacks and hybrid membranes for water purification and desalination.

Materials	Pore preparation method	Tested solution	Water flux	Application	Pore size	Reference
SLG [a]	Oxygen plasma etching	K^+, Na^+, Li^+, Cl^-	70 g m^{-2} s^{-1} atm^{-1}	Water purification	0,5-1 nm	[19b]
FLG [b]	Electron beam irradiation (SEM)	-----	-----	-----	~6 nm	[52]
MLG [c]	Electron beam irradiation (TEM)	-----	-----	-----	~3,5 nm	[53]
SLG/FLG	Thermal oxidation etching	-----	-----	-----	20-180 nm	[56]
SLG/FLG/ MLG	Ozone etching	-----	-----	-----	2-6 nm	[57]
SLG	Chemical etching	K^+, Cl^-, Allura red	-----	Ionic transport	0,2-0,4 nm	[19a]
SLG/ PVDF [d]	Filtration	Organic dyes	21,6 L m^{-2} h^{-1} bar^{-1}	Water purification	~0,2 nm	[15a]

GO-UiO66 [e]	Filtration	Rhodamine B	~15 L m^{-2} h^{-1} bar^{-1}	Water purification	~0,4 nm	[67]
rGO-UiO66	Filtration	Rhodamine B	~30 L m^{-2} h^{-1} bar^{-1}	Water purification	~0,4 nm	[67]
MLGO [f]	Drop-casting	Cu^{2+}, Mn^{2+}, Cd^{2+}, Na^{+}, RhB,	-----	Water purification	<10 nm	[60b]
MLGO	Drop-casting	K^{+}, Na^{+}, Li^{+}, Mg^{2+}, Ca^{2+},	0,36 L m^{-2} h^{-1} bar^{-1}	Ion sieving	-----	[61]
GO/TMC [g]	Impregnation	MB[h]	27,6 L m^{-2} h^{-1} bar^{-1}	Water purification	few nm	[81]
MLGO	Spin and spray coating	-----	-----	Water purification	~0,5 nm	[64]
GO/HPEI[i]	Surface coating	-----	-----	CO_2 capture	-----	[46]
GO-PAH [j]	Surface coating	Mg^{2+}, Cl^{-}, sucrose	19 L m^{-2} h^{-1} bar^{-1}	Water purification	~1 nm	[82]
rGO-CNT[k]	Vacuum filtration	Organic dyes	20-30 L m^{-2} h^{-1} bar^{-1}	Water purification	-----	[68]
GO-CS[l]	Electrospinning	Cu^{2+}, Pb^{2+}, Cr^{6+}	-----	Water purification	-----	[89]
MoS_2	Electron beam irradiation (TEM)	-----	-----	Detection DNA translocation	2-20 nm	[54]
MoS_2	Electron beam irradiation (TEM)	------	-----	Nanopower generator	2-6 nm	[29b]
MoS_2	Vacuum filtration	Organic dyes	245 L m^{-2} h^{-1} bar^{-1}	Water purification	<3 nm	[69]
MoS_2/Pebax	Spin coating	-----	-----	Gasoline desulfurization	~0,3 nm	[65a]
WS_2	Vacuum filtration	Organic dyes	730 L m^{-2} h^{-1} bar^{-1}	Water purification	<3 nm	[70]
GO/PA[m]	LbL deposition	Na^{+}, Cl^{-}	14 L m^{-2} h^{-1} bar^{-1}	Water purification	<1 nn	[79]
GO-PA	Interfacial polymerization	Na^{+}, Ca^{2+}, Cl^{-}	85 L m^{-2} h^{-1} bar^{-1}	Water purification	-----	[76]
GO-PA	Interfacial polymerization	Na^{+} Cl^{-}, SO_4^{2-}	59.4 m^{-2} h^{-1} bar^{-1}	Water purification	-----	[75]
MXene	Filtration	Mg^{2+}, Na^{+}, MB	37,4 m^{-2} h^{-1} bar^{-1}	Water purification	0,3-0,6 nm	[94]

[a] single layer graphene, [b] few layers graphene (<10), [c] multi layers graphene (>10), [d] polyvinylidene fluoride reduced, [e] zirconium metal organic frameworks made up of $[Zr_6O_4(OH)_4]$ clusters, [f] multi layers graphene oxide, [g] 1,3,5-benzenetricarbonyl trichloride, [h] methylene blue, [i] hyperbranched polyethylenimine, [j] poly(allylamine hydrochloride), [k] carbon nanotubes, [l] chitosan, [m] polyamide,

Table 2. Two-dimensional materials-based membranes and electrodes used in Reverse Electrodialysis.

Membrane	Electrolyte	Electrode	Power density	Ref.
Porous graphene	NaCl	Ag/AgCl	1.15 W m^{-2}	[112]
AEM[a]	NaCl	Graphene hydrogel	482.4 mW m^{-2}	[113]
GO[b]	KCl	Ag/AgCl	-----	[146]
Single layer MoS_2[c]	KCl	Ag/AgCl	10^6 W m^{-2}	[29b]
CEM[d]**/AEM**	NaCl	MoS_2	0.2 W m^{-2}	[147]
CEM/AEM	NaCl	MoS_2-porous carbon	~0.48 W m^{-2}	[14]

[a] anion exchange membrane, [b] graphene oxide, [c] molybdenum disulfide, [d] cation exchange membrane.

The table of contents

Two-dimensional materials (2DMs) possess unique features that make them ideal for the realization of stable, selective, ultra-thin membranes for *blue energy* harvesting, as well as for water purification technologies. In this review, we highlight recent developments on the fabrication and the use of atomically-thin 2DMs-based membranes, with particular attention on Pressure Retarded Osmosis (PRO) and Reverse Electrodialysis (RED) processes.

Title Atom-thick membranes for water purification and blue energy harvesting

ToC figure

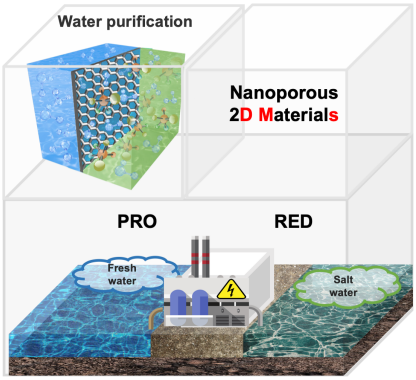

References

[1] a) D. Griggs, M. Stafford-Smith, O. Gaffney, J. Rockström, M. C. Öhman, P. Shyamsundar, W. Steffen, G. Glaser, N. Kanie, I. Noble, *Nature* **2013**, 495, 305; b) S. Chu, A. Majumdar, *Nature* **2012**, 488, 294; c) J. C. Crittenden, H. S. White, *J. Am. Chem. Soc.* **2010**, 132, 4503.
[2] https://www.iea.org/renewables2018/, *Market Report Series: Renewables 2018 – Analysis and Forecast to 2023* ISBN 978-92-64-30684-4.
[3] D.A. Mc Quarrie, J. D. Simon, *Physical Chemistry – A molecular approach, University Science Books* **1997**, *Sausalito, California*.

[4] a) J. W. Post, J. Veerman, H. V. M. Hamelers, G. J. W. Euverink, S. J. Metz, K. Nymeijer, C. J. N. Buisman, *J. Membr. Sci.* **2007**, 288, 218; b) R. A. Tufa, S. Pawlowski, J. Veerman, K. Bouzek, E. Fontananova, G. di Profio, S. Velizarov, J. G. Crespo, K. Nijmeijer, E. Curcio, *Appl. Energy* **2018**, 225, 290.
[5] a) O. Schaetzle, C. J. N. Buisman, *Engineering* **2015**, 1, 164; b) M. Kurihara, M. Hanakawa, *Desalination* **2013**, 308, 131.
[6] N. Y. Yip, D. Brogioli, H. V. M. Hamelers, K. Nijmeijer, *Environ. Sci. Technol.* **2016**, 50, 12072.
[7] X. Wang, P. L. McCarty, J. Liu, N.-Q. Ren, D.-J. Lee, H.-Q. Yu, Y. Qian, J. Qu, *Proc. Natl. Acad. Sci.* **2015**, 112, 1630.
[8] F. Helfer, C. Lemckert, Y. G. Anissimov, *J. Membr. Sci.* **2014**, 453, 337.
[9] B. E. Logan, M. Elimelech, *Nature* **2012**, 488, 313.
[10] Z. Jia, B. Wang, S. Song, Y. Fan, *Renewable and Sustainable Energy Rev.* **2014**, 31, 91.
[11] G. Z. Ramon, B. J. Feinberg, E. M. V. Hoek, *Energy Environ. Sci.* **2011**, 4, 4423.
[12] *https://www.who.int/topics/drinking_water/en/* **2019**.
[13] K. S. Novoselov, A. K. Geim, S. V. Morozov, D. Jiang, Y. Zhang, S. V. Dubonos, I. V. Grigorieva, A. A. Firsov, *Science* **2004**, 306, 666.
[14] A. C. Ferrari, F. Bonaccorso, V. Fal'ko, K. S. Novoselov, S. Roche, P. Bøggild, S. Borini, F. H. L. Koppens, V. Palermo, N. Pugno, J. A. Garrido, R. Sordan, A. Bianco, L. Ballerini, M. Prato, E. Lidorikis, J. Kivioja, C. Marinelli, T. Ryhänen, A. Morpurgo, J. N. Coleman, V. Nicolosi, L. Colombo, A. Fert, M. Garcia-Hernandez, A. Bachtold, G. F. Schneider, F. Guinea, C. Dekker, M. Barbone, Z. Sun, C. Galiotis, A. N. Grigorenko, G. Konstantatos, A. Kis, M. Katsnelson, L. Vandersypen, A. Loiseau, V. Morandi, D. Neumaier, E. Treossi, V. Pellegrini, M. Polini, A. Tredicucci, G. M. Williams, B. Hee Hong, J.-H. Ahn, J. Min Kim, H. Zirath, B. J. van Wees, H. van der Zant, L. Occhipinti, A. Di Matteo, I. A. Kinloch, T. Seyller, E. Quesnel, X. Feng, K. Teo, N. Rupesinghe, P. Hakonen, S. R. T. Neil, Q. Tannock, T. Löfwander, J. Kinaret, *Nanoscale* **2015**, 7, 4598.
[15] a) Y. Han, Z. Xu, C. Gao, *Adv. Funct. Mater.* **2013**, 23, 3693; b) Y. Ying, W. Ying, Q. Li, D. Meng, G. Ren, R. Yan, X. Peng, *Appl. Mater. Today* **2017**, 7, 144; c) M. A. Shannon, P. W. Bohn, M. Elimelech, J. G. Georgiadis, B. J. Mariñas, A. M. Mayes, *Nature* **2008**, 452, 301; d) D. Cohen-Tanugi, J. C. Grossman, *Nano Lett.* **2012**, 12, 3602; e) S. Dervin, D. D. Dionysiou, S. C. Pillai, *Nanoscale* **2016**, 8, 15115; f) T. Posati, M. Nocchetti, A. Kovtun, A. Donnadio, M. Zambianchi, A. Aluigi, M. L. Capobianco, F. Corticelli, V. Palermo, G. Ruani, R. Zamboni, M. L. Navacchia, M. Melucci, *ACS Omega* **2019**, 4, 4839.
[16] a) C. Anichini, W. Czepa, D. Pakulski, A. Aliprandi, A. Ciesielski, P. Samorì, *Chem. Soc. Rev.* **2018**, 47, 4860; b) L. Wang, M. S. H. Boutilier, P. R. Kidambi, D. Jang, N. G. Hadjiconstantinou, R. Karnik, *Nat. Nanotechnol.* **2017**, 12, 509; c) K. Celebi, J. Buchheim, R. M. Wyss, A. Droudian, P. Gasser, I. Shorubalko, J. I. Kye, C. Lee, H. G. Park, *Science* **2014**, 344, 289.
[17] a) Z. Zhang, X. Sui, P. Li, G. Xie, X.-Y. Kong, K. Xiao, L. Gao, L. Wen, L. Jiang, *J. Am. Chem. Soc.* **2017**, 139, 8905; b) L. Cao, Q. Wen, Y. Feng, D. Ji, H. Li, N. Li, L. Jiang, W. Guo, *Adv. Funct. Mater.* **2018**, 28, 1804189; c) A. Aliprandi, D. Pakulski, A. Ciesielski, P. Samorì, *ACS Nano* **2017**, 11, 10654; d) A. Siria, M.-L. Bocquet, L. Bocquet, *Nature Rev. Chem.* **2017**, 1, 0091; e) G. Anagnostopoulos, G. Paterakis, I. Polyzos, P.-N. Pappas, K. Kouroupis-Agalou, N. Mirotta, A. Scidà, V. Palermo, J. Parthenios, K. Papagelis, C. Galiotis, *ACS Appl. Mater. Interfaces* **2018**, 10, 43192; f) Z. Y. Xia, D. Wei, E. Anitowska, V. Bellani, L. Ortolani, V. Morandi, M. Gazzano, A. Zanelli, S. Borini, V. Palermo, *Carbon* **2015**, 84, 254; g) A. Ansaldo, P. Bondavalli, S. Bellani, A. E. Del Rio Castillo, M. Prato, V. Pellegrini, G. Pognon, F. Bonaccorso, *ChemNanoMat* **2017**, 3, 436; h) F. Torrisi, T. Hasan, W. Wu, Z.

Sun, A. Lombardo, T. S. Kulmala, G.-W. Hsieh, S. Jung, F. Bonaccorso, P. J. Paul, D. Chu, A. C. Ferrari, *ACS Nano* **2012**, 6, 2992.
[18] a) H. Li, Z. Song, X. Zhang, Y. Huang, S. Li, Y. Mao, H. J. Ploehn, Y. Bao, M. Yu, *Science* **2013**, 342, 95; b) K. Celebi, J. Buchheim, R. M. Wyss, A. Droudian, P. Gasser, I. Shorubalko, J.-I. Kye, C. Lee, H. G. Park, *Science* **2014**, 344, 289; c) S. P. Koenig, L. Wang, J. Pellegrino, J. S. Bunch, *Nat. Nanotechnol.* **2012**, 7, 728; d) M. Donarelli, S. Prezioso, F. Perrozzi, L. Giancaterini, C. Cantalini, E. Treossi, V. Palermo, S. Santucci, L. Ottaviano, *2D Materials* **2015**, 2, 035018.
[19] a) S. C. O'Hern, M. S. H. Boutilier, J.-C. Idrobo, Y. Song, J. Kong, T. Laoui, M. Atieh, R. Karnik, *Nano Lett.* **2014**, 14, 1234; b) S. P. Surwade, S. N. Smirnov, I. V. Vlassiouk, R. R. Unocic, G. M. Veith, S. Dai, S. M. Mahurin, *Nat. Nanotechnol.* **2015**, 10, 459; c) W. Sparreboom, A. van den Berg, J. C. T. Eijkel, *Nat. Nanotechnol.* **2009**, 4, 713.
[20] a) J. Zhu, J. Hou, A. Uliana, Y. Zhang, M. Tian, B. Van der Bruggen, *J. Mater. Chem. A* **2018**, 6, 3773; b) Y. Zhao, Y. Xie, Z. Liu, X. Wang, Y. Chai, F. Yan, *Small* **2014**, 10, 4521; c) G. Liu, W. Jin, N. Xu, *Angew. Chem. Int. Ed.* **2016**, 55, 13384.
[21] a) L. Eykens, K. De Sitter, C. Dotremont, L. Pinoy, B. Van der Bruggen, *Sep. Purif. Technol.* **2017**, 182, 36; b) B. S. Lalia, V. Kochkodan, R. Hashaikeh, N. Hilal, *Desalination* **2013**, 326, 77; c) J. J. Keating, J. Imbrogno, G. Belfort, *ACS Appl. Mater. Interfaces* **2016**, 8, 28383; d) M. Khodakarami, L. Alagha, *Polym. Plast. Technol.* **2017**, 56, 2019.
[22] a) J. R. Li, J. Sculley, H. C. Zhou, *Chem. Rev.* **2012**, 112, 869; b) S. L. Qiu, M. Xue, G. S. Zhu, *Chem. Soc. Rev.* **2014**, 43, 6116; c) C. H. Wang, X. L. Liu, N. K. Demir, J. P. Chen, K. Li, *Chem. Soc. Rev.* **2016**, 45, 5107.
[23] a) Z. Lai, G. Bonilla, I. Diaz, J. G. Nery, K. Sujaoti, M. A. Amat, E. Kokkoli, O. Terasaki, R. W. Thompson, M. Tsapatsis, D. G. Vlachos, *Science* **2003**, 300, 456; b) C. M. Lew, R. Cai, Y. S. Yan, *Acc. Chem. Res.* **2010**, 43, 210.
[24] Q. Z. Wang, N. Li, B. Bolto, M. Hoang, Z. L. Xie, *Desalination* **2016**, 387, 46.
[25] a) W. Cheng, M. J. Campolongo, S. J. Tan, D. Luo, *Nano Today* **2009**, 4, 482; b) S. Drieschner, M. Weber, J. Wohlketzetter, J. Vieten, E. Makrygiannis, B. M. Blaschke, V. Morandi, L. Colombo, F. Bonaccorso, J. A. Garrido, *2D Materials* **2016**, 3, 045013.
[26] a) M. G. Buonomenna, *RSC Adv.* **2013**, 3, 5694; b) G. Amy, N. Ghaffour, Z. Li, L. Francis, R. V. Linares, T. Missimer, S. Lattemann, *Desalination* **2017**, 401, 16; c) W.-g. Kim, S. Nair, *Chem. Eng. Sci.* **2013**, 104, 908; d) G. Liu, W. Jin, N. Xu, *Angew. Chem. Int. Ed.* **2016**, 55, 13384; e) Z. Wang, A. Wu, L. C. Ciacchi, G. Wei, *Nanomaterials* **2018**, 8, 65.
[27] a) K. A. DeFriend, M. R. Wiesner, A. R. Barron, *J. Membr. Sci.* **2003**, 224, 11; b) X. P. Cao, D. Li, W. H. Jing, W. H. Xing, Y. Q. Fan, *J. Mater. Chem.* **2012**, 22, 15309.
[28] a) M. S. Rahaman, C. D. Vecitis, M. Elimelech, *Environ. Sci. Technol.* **2012**, 46, 1556; b) Q. Xu, H. Xu, J. Chen, Y. Lv, C. Dong, T. S. Sreeprasad, *Inorg. Chem. Front.* **2015**, 2, 417.
[29] a) Z. Zheng, R. Grünker, X. Feng, *Adv. Matter.* **2016**, 28, 6529; b) J. Feng, M. Graf, K. Liu, D. Ovchinnikov, D. Dumcenco, M. Heiranian, V. Nandigana, N. R. Aluru, A. Kis, A. Radenovic, *Nature* **2016**, 536, 197.
[30] a) T. Shibutani, T. Kitaura, Y. Ohmukai, T. Maruyama, S. Nakatsuka, T. Watabe, H. Matsuyama, *J. Membr. Sci.* **2011**, 376, 102; b) E. Saljoughi, S. M. Mousavi, *Sep. Purif. Technol.* **2012**, 90, 22; c) M. H. Liu, Q. Chen, L. Z. Wang, S. C. Yu, C. J. Gao, *Desalination* **2015**, 367, 11; d) F. Liu, N. A. Hashim, Y. Liu, M. R. M. Abed, K. Li, *J. Membr. Sci.* **2011**, 375, 1.
[31] a) X. Zhao, P. Zhang, Y. Chen, Z. Su, G. Wei, *Nanoscale* **2015**, 7, 5080; b) W. J. Lau, A. F. Ismail, N. Misdan, M. A. Kassim, *Desalination* **2012**, 287, 190; c) Z. Wang, A. Wu, L. Colombi Ciacchi, G. Wei, *Nanomater.* **2018**, 8, 65.
[32] a) N. Y. Yip, M. Elimelech, *Environ. Sci. Technol.* **2011**, 45, 10273; b) A. Achilli, T. Y. Cath, A. E. Childress, *J. Membr. Sci.* **2009**, 343, 42.

[33] M. E. Suk, N. R. Aluru, *J. Phys. Chem. Lett.* **2010**, 1, 1590.
[34] R. Zhang, Y. Liu, M. He, Y. Su, X. Zhao, M. Elimelech, Z. Jiang, *Chem. Soc. Rev.* **2016**, 45, 5888.
[35] a) P. S. Goh, W. J. Lau, M. H. D. Othman, A. F. Ismail, *Desalination* **2018**, 425, 130; b) X. Zhao, R. Zhang, Y. Liu, M. He, Y. Su, C. Gao, Z. Jiang, *J. Membr. Sci.* **2018**, 551, 145.
[36] X. Wang, Y. Zhao, E. Tian, J. Li, Y. Ren, *Adv. Mater. Interfaces* **2018**, 5, 1701427.
[37] D. H. Seo, S. Pineda, Y. C. Woo, M. Xie, A. T. Murdock, E. Y. M. Ang, Y. Jiao, M. J. Park, S. I. Lim, M. Lawn, F. F. Borghi, Z. J. Han, S. Gray, G. Millar, A. Du, H. K. Shon, T. Y. Ng, K. Ostrikov, *Nat. Commun.* **2018**, 9, 683.
[38] a) C. Lee, X. Wei, J. W. Kysar, J. Hone, *Science* **2008**, 321, 385; b) G. R. Bhimanapati, Z. Lin, V. Meunier, Y. Jung, J. Cha, S. Das, D. Xiao, Y. Son, M. S. Strano, V. R. Cooper, L. Liang, S. G. Louie, E. Ringe, W. Zhou, S. S. Kim, R. R. Naik, B. G. Sumpter, H. Terrones, F. Xia, Y. Wang, J. Zhu, D. Akinwande, N. Alem, J. A. Schuller, R. E. Schaak, M. Terrones, J. A. Robinson, *ACS Nano* **2015**, 9, 11509.
[39] a) C. Tan, X. Cao, X. J. Wu, Q. He, J. Yang, X. Zhang, J. Chen, W. Zhao, S. Han, G. H. Nam, M. Sindoro, H. Zhang, *Chem. Rev.* **2017**, 117, 6225; b) S. Z. Butler, S. M. Hollen, L. Cao, Y. Cui, J. A. Gupta, H. R. Gutiérrez, T. F. Heinz, S. S. Hong, J. Huang, A. F. Ismach, E. Johnston-Halperin, M. Kuno, V. V. Plashnitsa, R. D. Robinson, R. S. Ruoff, S. Salahuddin, J. Shan, L. Shi, M. G. Spencer, M. Terrones, W. Windl, J. E. Goldberger, *ACS Nano* **2013**, 7, 2898.
[40] a) S. Garaj, W. Hubbard, A. Reina, J. Kong, D. Branton, J. A. Golovchenko, *Nature* **2010**, 467, 190; b) C. A. Merchant, K. Healy, M. Wanunu, V. Ray, N. Peterman, J. Bartel, M. D. Fischbein, K. Venta, Z. Luo, A. T. C. Johnson, M. Drndić, *Nano Lett.* **2010**, 10, 2915; c) X. Han, M. R. Funk, F. Shen, Y.-C. Chen, Y. Li, C. J. Campbell, J. Dai, X. Yang, J.-W. Kim, Y. Liao, J. W. Connell, V. Barone, Z. Chen, Y. Lin, L. Hu, *ACS Nano* **2014**, 8, 8255; d) T. H. Han, Y.-K. Huang, A. T. L. Tan, V. P. Dravid, J. Huang, *J. Am. Chem. Soc.* **2011**, 133, 15264; e) Y. Zhu, S. Murali, M. D. Stoller, K. J. Ganesh, W. Cai, P. J. Ferreira, A. Pirkle, R. M. Wallace, K. A. Cychosz, M. Thommes, D. Su, E. A. Stach, R. S. Ruoff, *Science* **2011**, 332, 1537; f) O. Akhavan, E. Ghaderi, *Small* **2013**, 9, 3593.
[41] G. Diankov, M. Neumann, D. Goldhaber-Gordon, *ACS Nano* **2013**, 7, 1324.
[42] a) W. Zhang, Y. Zhu, X. Liu, D. Wang, J. Li, L. Jiang, J. Jin, *Angew. Chem. Int. Ed.* **2014**, 53, 856; b) B. M. Ganesh, A. M. Isloor, A. F. Ismail, *Desalination* **2013**, 313, 199.
[43] a) B. Khorshidi, T. Thundat, B. A. Fleck, M. Sadrzadeh, *Sci. Rep.* **2016**, 6, 22069; b) B. Khorshidi, T. Thundat, B. A. Fleck, M. Sadrzadeh, *RSC Adv.* **2015**, 5, 54985.
[44] a) M. Zhang, X. Zhao, G. Zhang, G. Wei, Z. Su, *J. Mater. Chem. B* **2017**, 5, 1699; b) H. R. Pant, H. J. Kim, M. K. Joshi, B. Pant, C. H. Park, J. I. Kim, K. S. Hui, C. S. Kim, *J. Hazard. Mater.* **2014**, 264, 25.
[45] P. K. S. Mural, A. Banerjee, M. S. Rana, A. Shukla, B. Padmanabhan, S. Bhadra, G. Madras, S. Bose, *J. Mater. Chem. A* **2014**, 2, 17635.
[46] Y. Shen, H. Wang, J. Liu, Y. Zhang, *ACS Sustainable Chem. Eng.* **2015**, 3, 1819.
[47] G.-R. Xu, S.-H. Wang, H.-L. Zhao, S.-B. Wu, J.-M. Xu, L. Li, X.-Y. Liu, *J. Membr. Sci.* **2015**, 493, 428.
[48] a) A. Ciesielski, P. Samorì, *Chem. Soc. Rev*. **2014**, 43, 381; b) A. Ciesielski, P. Samorì, *Adv. Mater*. **2016**, 28, 6030; c) S. Witomska, T. Leydecker, A. Ciesielski, P. Samorì, *Adv. Funct. Mater.* **2019**, DOI: 10.1002/adfm.201901126.
[49] P. R. Kidambi, D. D. Mariappan, N. T. Dee, A. Vyatskikh, S. Zhang, R. Karnik, A. J. Hart, *ACS Appl. Mater. Interfaces* **2018**, 10, 10369.
[50] a) S. A. Akimov, P. E. Volynsky, T. R. Galimzyanov, P. I. Kuzmin, K. V. Pavlov, O. V. Batishchev, *Sci. Rep.* **2017**, 7; b) W. F. D. Bennett, N. Sapay, D. P. Tieleman, *Biophys. J.* **2014**, 106, 210; c) S. A. Akimov, P. E. Volynsky, T. R. Galimzyanov, P. I. Kuzmin, K. V. Pavlov, O. V. Batishchev, *Sci. Rep.* **2017**, 7.

[51] L. Prozorovska, P. R. Kidambi, *Adv. Mater.* **2018**, 30, 1801179.
[52] D. Fox, A. O'Neill, D. Zhou, M. Boese, J. N. Coleman, H. Z. Zhang, *Appl. Phys. Lett.* **2011**, 98, 243117.
[53] M. D. Fischbein, M. Drndić, *Appl. Phys. Lett.* **2008**, 93, 113107.
[54] K. Liu, J. Feng, A. Kis, A. Radenovic, *ACS Nano* **2014**, 8, 2504.
[55] A. Siria, P. Poncharal, A.-L. Biance, R. Fulcrand, X. Blase, S. T. Purcell, L. Bocquet, *Nature* **2013**, 494, 455.
[56] L. Liu, S. Ryu, M. R. Tomasik, E. Stolyarova, N. Jung, M. S. Hybertsen, M. L. Steigerwald, L. E. Brus, G. W. Flynn, *Nano Lett.* **2008**, 8, 1965.
[57] H. Tao, J. Moser, F. Alzina, Q. Wang, C. M. Sotomayor-Torres, *J. Phys. Chem. C* **2011**, 115, 18257.
[58] a) A. A. Ramanathan, M. W. Aqra, A. E. J. E. C. L. Al-Rawajfeh, *Environ. Chem. Lett.* **2018**, 16, 1217; b) C. Li, S. M. Meckler, Z. P. Smith, J. E. Bachman, L. Maserati, J. R. Long, B. A. Helms, *Adv. Mater.* **2018**, 30, 1704953.
[59] Y.-C. Wang, S. R. Kumar, C.-M. Shih, W.-S. Hung, Q.-F. An, H.-C. Hsu, S.-H. Huang, S. J. Lue, *J. Membr. Sci.* **2017**, 540, 391.
[60] a) H. W. Kim, H. W. Yoon, S.-M. Yoon, B. M. Yoo, B. K. Ahn, Y. H. Cho, H. J. Shin, H. Yang, U. Paik, S. Kwon, J.-Y. Choi, H. B. Park, *Science* **2013**, 342, 91; b) P. Sun, M. Zhu, K. Wang, M. Zhong, J. Wei, D. Wu, Z. Xu, H. Zhu, *ACS Nano* **2013**, 7, 428.
[61] L. Chen, G. Shi, J. Shen, B. Peng, B. Zhang, Y. Wang, F. Bian, J. Wang, D. Li, Z. Qian, G. Xu, G. Liu, J. Zeng, L. Zhang, Y. Yang, G. Zhou, M. Wu, W. Jin, J. Li, H. Fang, *Nature* **2017**, 550, 380.
[62] D. B. Hall, P. Underhill, J. M. Torkelson, *Polym. Eng. Sci.* **1998**, 38, 2039.
[63] a) H. Yan, Z. H. Chen, Y. Zheng, C. Newman, J. R. Quinn, F. Dotz, M. Kastler, A. Facchetti, *Nature* **2009**, 457, 679; b) W. Rekab, M. A. Stoeckel, M. El Gemayel, M. Gobbi, E. Orgiu, P. Samorì, *ACS Appl. Mater. Interfaces* **2016**, 8, 9829; c) T. Leydecker, M. Eredia, F. Liscio, S. Milita, G. Melinte, O. Ersen, M. Sommer, A. Ciesielski, P. Samorì, *Carbon* **2018**, 130, 495; d) H. A. Becerril, J. Mao, Z. Liu, R. M. Stoltenberg, Z. Bao, Y. Chen, *ACS Nano* **2008**, 2, 463.
[64] R. R. Nair, H. A. Wu, P. N. Jayaram, I. V. Grigorieva, A. K. Geim, *Science* **2012**, 335, 442.
[65] a) F. Pan, H. Ding, W. Li, Y. Song, H. Yang, H. Wu, Z. Jiang, B. Wang, X. Cao, *J. Membr. Sci.* **2018**, 545, 29; b) K. Cao, Z. Jiang, J. Zhao, C. Zhao, C. Gao, F. Pan, B. Wang, X. Cao, J. Yang, *J. Membr. Sci.* **2014**, 469, 272.
[66] a) D. A. Dikin, S. Stankovich, E. J. Zimney, R. D. Piner, G. H. B. Dommett, G. Evmenenko, S. T. Nguyen, R. S. Ruoff, *Nature* **2007**, 448, 457; b) M. Chhowalla, H. S. Shin, G. Eda, L.-J. Li, K. P. Loh, H. Zhang, *Nat. Chem.* **2013**, 5, 263.
[67] K. Guan, D. Zhao, M. Zhang, J. Shen, G. Zhou, G. Liu, W. Jin, *J. Membr. Sci.* **2017**, 542, 41.
[68] X. Chen, M. Qiu, H. Ding, K. Fu, Y. Fan, *Nanoscale* **2016**, 8, 5696.
[69] L. Sun, H. Huang, X. Peng, *Chem. Commun.* **2013**, 49, 10718.
[70] L. Sun, Y. Ying, H. Huang, Z. Song, Y. Mao, Z. Xu, X. Peng, *ACS Nano* **2014**, 8, 6304.
[71] a) W. J. Lau, S. Gray, T. Matsuura, D. Emadzadeh, J. Paul Chen, A. F. Ismail, *Water Res.* **2015**, 80, 306; b) A. W. Mohammad, Y. H. Teow, W. L. Ang, Y. T. Chung, D. L. Oatley-Radcliffe, N. Hilal, *Desalination* **2015**, 356, 226; c) B. Khorshidi, T. Thundat, D. Pernitsky, M. Sadrzadeh, *J. Membr. Sci.* **2017**, 535, 248.
[72] J. E. Cadotte, R. J. Petersen, R. E. Larson, E. E. Erickson, *Desalination* **1980**, 32, 25.
[73] J. Cadotte, R. Forester, M. Kim, R. Petersen, T. Stocker, *Desalination* **1988**, 70, 77.
[74] a) A. K. Ghosh, B.-H. Jeong, X. Huang, E. M. V. Hoek, *J. Membr. Sci.* **2008**, 311, 34; b) I. J. Roh, A. R. Greenberg, V. P. Khare, *Desalination* **2006**, 191, 279.

[75] J. Yin, G. Zhu, B. Deng, *Desalination* **2016**, 379, 93.
[76] S. Bano, A. Mahmood, S.-J. Kim, K.-H. Lee, *J. Mater. Chem. A* **2015**, 3, 2065.
[77] G. Decher, *Science* **1997**, 277, 1232.
[78] a) D. D. Kulkarni, I. Choi, S. Singamaneni, V. V. Tsukruk, *Acs Nano* **2010**, 4, 4667; b) T. Lee, S. H. Min, M. Gu, Y. K. Jung, W. Lee, J. U. Lee, D. G. Seong, B. S. Kim, *Chem. Mater.* **2015**, 27, 3785.
[79] W. Choi, J. Choi, J. Bang, J.-H. Lee, *ACS Appl. Mater. Interfaces* **2013**, 5, 12510.
[80] X. Wang, H. Bai, G. Shi, *J. Am. Chem. Soc.* **2011**, 133, 6338.
[81] M. Hu, B. Mi, *Environ. Sci. Technol.* **2013**, 47, 3715.
[82] M. Hu, B. Mi, *J. Membr. Sci.* **2014**, 469, 80.
[83] a) D. H. Reneker, I. Chun, *Nanotechnology* **1996**, 7, 216; b) A. Frenot, I. S. Chronakis, *Curr. Opi. Colloid Interface Sci.* **2003**, 8, 64.
[84] Zeleny John, *Phys. Rev.* 3, 69.
[85] F. A., *US Patent Specification 1975504* **1934**.
[86] H. Ke, E. Feldman, P. Guzman, J. Cole, Q. Wei, B. Chu, A. Alkhudhiri, R. Alrasheed, B. S. Hsiao, *J. Membr. Sci.* **2016**, 515, 86.
[87] M. Faccini, G. Borja, M. Boerrigter, D. Morillo Martìn, S. Martìnez Crespiera, S. Vázquez-Campos, L. Aubouy, D. Amantia, *J. Nanomater.* **2015**, 2015, 9.
[88] W. Jang, J. Yun, K. Jeon, H. Byun, *RSC Adv.* **2015**, 5, 46711.
[89] H. Hadi Najafabadi, M. Irani, L. Roshanfekr Rad, A. Heydari Haratameh, I. Haririan, *RSC Adv.* **2015**, 5, 16532.
[90] N. O. San, A. Celebioglu, Y. Tümtaş, T. Uyar, T. Tekinay, *RSC Adv.* **2014**, 4, 32249.
[91] T. C. Mokhena, A. S. Luyt, *J. Clean. Prod.* **2017**, 156, 470.
[92] J. Wang, P. Zhang, B. Liang, Y. Liu, T. Xu, L. Wang, B. Cao, K. Pan, *ACS Appl. Mater. Interfaces* **2016**, 8, 6211.
[93] C. Feng, K. C. Khulbe, T. Matsuura, R. Gopal, S. Kaur, S. Ramakrishna, M. Khayet, *J. Membr. Sci.* **2008**, 311, 1.
[94] C. E. Ren, K. B. Hatzell, M. Alhabeb, Z. Ling, K. A. Mahmoud, Y. Gogotsi, *J. Phys. Chem. Lett.* **2015**, 6, 4026.
[95] Z. Wang, R. Sahadevan, C.-N. Yeh, T. J. Menkhaus, J. Huang, H. Fong, *Nanotechnology* **2017**, 28, 31LT02.
[96] R. W. Baker, B. T. Low, *Macromolecules* **2014**, 47, 6999.
[97] J.-P. Bouchaud, A. Georges, *Phys. Rep.* **1990**, 195, 127.
[98] G. M. Geise, H.-S. Lee, D. J. Miller, B. D. Freeman, J. E. McGrath, D. R. Paul, *J. Polym. Sci. Polym. Phys.* **2010**, 48, 1685.
[99] D. D. Ganji, S. H. H. Kachapi, in *Application of Nonlinear Systems in Nanomechanics and Nanofluids*, DOI: https://doi.org/10.1016/B978-0-323-35237-6.00006-6 (Eds: D. D. Ganji, S. H. H. Kachapi), William Andrew Publishing, Oxford **2015**, p. 205.
[100] A. Szymczyk, P. Fievet, *J. Membr. Sci.* **2005**, 252, 77.
[101] a) L. Bocquet, E. Charlaix, *Chem. Soc. Rev.* **2010**, 39, 1073; b) A. Ajdari, L. Bocquet, *Phys. Rev. Lett.* **2006**, 96, 186102; c) C. Lee, C. Cottin-Bizonne, A.-L. Biance, P. Joseph, L. Bocquet, C. Ybert, *Phys. Rev. Lett.* **2014**, 112, 244501.
[102] M. I. Walker, K. Ubych, V. Saraswat, E. A. Chalklen, P. Braeuninger-Weimer, S. Caneva, R. S. Weatherup, S. Hofmann, U. F. Keyser, *ACS Nano* **2017**, 11, 1340.
[103] a) J. R. Werber, C. O. Osuji, M. Elimelech, *Nat. Rev. Mater.* **2016**, 1, 16018; b) S. C. O'Hern, M. S. H. Boutilier, J.-C. Idrobo, Y. Song, J. Kong, T. Laoui, M. Atieh, R. Karnik, *Nano Lett.* **2014**, 14, 1234; c) S. P. Koenig, L. Wang, J. Pellegrino, J. S. Bunch, *Nature Nanotechnol.* **2012**, 7, 728.
[104] N. Y. Yip, M. Elimelech, *Environ. Sci. Technol.* **2014**, 48, 11002.
[105] R. A. Tufa, S. Pawlowski, J. Veerman, K. Bouzek, E. Fontananova, G. di Profio, S. Velizarov, J. Goulão Crespo, K. Nijmeijer, E. Curcio, *Appl. Energ.* **2018**, 225, 290.

[106] a) M. Tedesco, H. V. M. Hamelers, P. M. Biesheuvel, *J. Memb. Sci.* **2018**, 565, 480; b) M. Tedesco, H. V. M. Hamelers, P. M. Biesheuvel, *J. Memb. Sci.* **2017**, 531, 172; c) M. Tedesco, H. V. M. Hamelers, P. M. Biesheuvel, *J. Memb. Sci.* **2016**, 510, 370.
[107] a) S. B. Lee, D. T. Mitchell, L. Trofin, T. K. Nevanen, H. Söderlund, C. R. Martin, *Science* **2002**, 296, 2198; b) A. L. Sisson, M. R. Shah, S. Bhosale, S. Matile, *Chem. Soc. Rev.* **2006**, 35, 1269; c) X. Hou, W. Guo, L. Jiang, *Chem. Soc. Rev.* **2011**, 40, 2385.
[108] D. H. Cho, K. H. Lee, Y. M. Kim, S. H. Park, W. H. Lee, S. M. Lee, Y. M. Lee, *Chem. Commun.* **2017**, 53, 2323.
[109] J. Veerman, M. Saakes, S. J. Metz, G. J. Harmsen, *J. Memb. Sci.* **2009**, 327, 136.
[110] J. Veerman, R. M. de Jong, M. Saakes, S. J. Metz, G. J. Harmsen, *J. Memb. Sci.* **2009**, 343, 7.
[111] a) F. Bonaccorso, L. Colombo, G. Yu, M. Stoller, V. Tozzini, A. C. Ferrari, R. S. Ruoff, V. Pellegrini, *Science* **2015**, 347, 1246501; b) S. Garaj, W. Hubbard, A. Reina, J. Kong, D. Branton, J. A. Golovchenko, *Nature* **2010**, 467; c) R. Raccichini, A. Varzi, S. Passerini, B. Scrosati, *Nature Mater.* **2014**, 14, 271; d) D. Jariwala, V. K. Sangwan, L. J. Lauhon, T. J. Marks, M. C. Hersam, *ACS Nano* **2014**, 8, 1102.
[112] J. Wan, L. Huang, J. Wu, L. Xiong, Z. Hu, H. Yu, T. Li, J. Zhou, *Adv. Funct. Mater.* **2018**, 28, 1800382.
[113] F. Zhan, Z. Wang, T. Wu, Q. Dong, C. Zhao, G. Wang, J. Qiu, *J. Mater. Chem. A* **2018**, 6, 4981.
[114] R. C. Rollings, A. T. Kuan, J. A. Golovchenko, *Nat. Commun.* **2016**, 7, 11408.
[115] X. Huang, X.-Y. Kong, L. Wen, L. Jiang, *Adv. Funct. Mater.* **2018**, 28, 1801079.
[116] H. Miedema, M. Vrouenraets, J. Wierenga, W. Meijberg, G. Robillard, B. Eisenberg, *Nano Lett.* **2007**, 7, 2886.
[117] D. Stein, M. Kruithof, C. Dekker, *Phys. Rev. Lett.* **2004**, 93, 035901.
[118] R. Karnik, C. Duan, K. Castelino, H. Daiguji, A. Majumdar, *Nano Lett.* **2007**, 7, 547.
[119] L.-J. Cheng, L. J. Guo, *Nano Lett.* **2007**, 7, 3165.
[120] F. H. J. van der Heyden, D. J. Bonthuis, D. Stein, C. Meyer, C. Dekker, *Nano Lett.* **2006**, 6, 2232.
[121] a) J. Ji, Q. Kang, Y. Zhou, Y. Feng, X. Chen, J. Yuan, W. Guo, Y. Wei, L. Jiang, *Adv. Funct. Mater.* **2017**, 27, 1603623; b) J. Gao, W. Guo, D. Feng, H. Wang, D. Zhao, L. Jiang, *J. Am. Chem. Soc.* **2014**, 136, 12265.
[122] R. Karnik, R. Fan, M. Yue, D. Li, P. Yang, A. Majumdar, *Nano Lett.* **2005**, 5, 943.
[123] J. L. B. Pirooz Mohazzabi, *J. Appl. Math. Phys.* **2017**, 5, 623.
[124] R. Long, Z. Kuang, Z. Liu, W. Liu, *Phys. Chem. Chem. Phys.* **2018**, 20, 7295.
[125] J. Hwang, S. Kataoka, A. Endo, H. Daiguji, *Lab Chip* **2016**, 16, 3824.
[126] J. Gao, W. Guo, D. Feng, H. Wang, D. Zhao, L. Jiang, *J. Am. Chem. Soc.* **2014**, 136, 12265.
[127] A. Esfandiar, B. Radha, F. C. Wang, Q. Yang, S. Hu, S. Garaj, R. R. Nair, A. K. Geim, K. Gopinadhan, *Science* **2017**, 358, 511.
[128] S. Hong, C. Constans, M. V. Surmani Martins, Y. C. Seow, J. A. Guevara Carrió, S. Garaj, *Nano Lett.* **2017**, 17, 728.
[129] J. Feng, K. Liu, M. Graf, D. Dumcenco, A. Kis, M. Di Ventra, A. Radenovic, *Nature Mater.* **2016**, 15, 850.
[130] T. Mouterde, A. Keerthi, A. R. Poggioli, S. A. Dar, A. Siria, A. K. Geim, L. Bocquet, B. Radha, *Nature* **2019**, 567, 87.
[131] N. Y. Yip, M. Elimelech, *Environ. Sci. Technol.* **2012**, 46, 5230.
[132] S. Loeb, R. S. Norman, *Science* **1975**, 189, 654.
[133] G. Han, S. Zhang, X. Li, T.-S. Chung, *J. Membr. Sci.* **2013**, 440, 108.
[134] a) K. Gerstandt, K. V. Peinemann, S. E. Skilhagen, T. Thorsen, T. Holt, *Desalination* **2008**, 224, 64; b) S. E. Skilhagen, *Desalin. Water Treat.* **2010**, 15, 271.

[135] C. Klaysom, T. Y. Cath, T. Depuydt, I. F. J. Vankelecom, *Chem. Soc. Rev.* **2013**, 42, 6959.
[136] a) N.-N. Bui, M. L. Lind, E. M. V. Hoek, J. R. McCutcheon, *J. Memb. Sci.* **2011**, 385-386, 10; b) N. Y. Yip, A. Tiraferri, W. A. Phillip, J. D. Schiffman, L. A. Hoover, Y. C. Kim, M. Elimelech, *Environ. Sci. Technol.* **2011**, 45, 4360.
[137] M. Elimelech, W. A. Phillip, *Science* **2011**, 333, 712.
[138] Z. Zheng, R. Grünker, X. Feng, *Adv. Mater.* **2016**, 28, 6529.
[139] a) P. Y. Huang, C. S. Ruiz-Vargas, A. M. van der Zande, W. S. Whitney, M. P. Levendorf, J. W. Kevek, S. Garg, J. S. Alden, C. J. Hustedt, Y. Zhu, J. Park, P. L. McEuen, D. A. Muller, *Nature* **2011**, 469, 389; b) R. K. Joshi, P. Carbone, F. C. Wang, V. G. Kravets, Y. Su, I. V. Grigorieva, H. A. Wu, A. K. Geim, R. R. Nair, *Science* **2014**, 343, 752.
[140] X. Tong, X. Wang, S. Liu, H. Gao, C. Xu, J. Crittenden, Y. Chen, *Carbon* **2018**, 138, 410.
[141] M. Hu, B. Mi, *J. Memb. Sci.* **2014**, 469, 80.
[142] S. Lim, M. J. Park, S. Phuntsho, A. Mai-Prochnow, A. B. Murphy, D. Seo, H. Shon, *J. Memb. Sci.* **2018**, 564, 382.
[143] A. Aliprandi, M. Eredia, C. Anichini, W. Baaziz, O. Ersen, A. Ciesielski, P. Samorì, *Chem. Commun.* **2019**, DOI: 10.1039/C9CC01822K.
[144] M. Sun, J. Li, *Nano Today* **2018**, 20, 121.
[145] M. F. Jimenez-Solomon, Q. Song, K. E. Jelfs, M. Munoz-Ibanez, L. A.G., *Nat. Mater.* **2016**, 15, 760.
[146] R. C. Rollings, A. T. Kuan, J. A. Golovchenko, *Nature Commun.* **2016**, 7, 11408.
[147] N. Jeong, H.-K. Kim, W.-S. Kim, J. Y. Choi, J.-H. Han, J.-Y. Nam, K. S. Hwang, S. Yang, E.-J. Jwa, T.-Y. Kim, S.-C. Park, Y.-S. Seo, S.-I. Kim, *Chem. Eng. J.* **2019**, 356, 292.